CrystEngComm

Accepted Manuscript

ROYAL SOCIETY OF CHEMISTRY

www.rsc.org/crystengcomm

Zinc and cadmium complexes based on bis-(1*H*-tetrazol-5-ylmethyl/ylethyl)-amine ligands: structures and photoluminescence properties

Duo-Zhi Wang* [a,b], Jian-Zhong Fan[b], Dian-Zeng Jia [a] and Ceng-Ceng Du[b]

[a]*Key Laboratory of Material and Technology for Clean Energy, Ministry of Education, Institute of Applied Chemistry, Xinjiang University, Urumqi, 830046 Xinjiang, P. R. China.*

[b]*College of Chemistry and Chemical Engineering, Xinjiang University, Urumqi 830046, P. R. China.*

* Corresponding authors. E-mail: wangdz@xju.edu.cn

To ***CrystEngComm***

Abstract The designed organic ligands bis-(1*H*-tetrazol-5-ylmethyl)-amine ($H_3\mathbf{L^1}$) and bis-(1*H*-tetrazol-5-ylethyl)-amine ($H_3\mathbf{L^2}$) have been successfully prepared and their coordination features have been explored. By the reaction of $H_3\mathbf{L^1}$ and $H_3\mathbf{L^2}$ with different zinc/cadmium salts, two 0D complexes $Cd_2(H\mathbf{L^1})_2(H_2O)_4\cdot 2H_2O$ (**4**), $Cd(H\mathbf{L^2})(H_2O)_3$ (**8**), seven new coordination polymers, $[Zn(H\mathbf{L^1})(H_2O)]_n$ (**1**), $[Zn(H\mathbf{L^1})]_n$ (**2**), $[Cd_3(H\mathbf{L^1})_2Cl_2]_n$ (**3**), $\{[Cd_2(H\mathbf{L^1})_2]\cdot H_2O\}_n$ (**5**), $[Zn(H\mathbf{L^2})]_n$ (**6**), $[Zn_2(H\mathbf{L^2})N_3Cl]_n$ (**7**) and $[Cd_2(H_2\mathbf{L^2})(NO_3)(OH)(H_2O)_2]_n$ (**9**) have been synthesized. All the compounds were fully characterized by elemental analysis, IR spectroscopy, thermogravimetric analysis, powder X-ray diffraction and single-crystal X-ray diffraction. Complex **4** exhibits a dinuclear structure, **8** represents a mononuclear structure. Besides, **4** and **8** are further assembled to form three-dimensional (3D) and two-dimensional (2D) supramolecular frameworks by hydrogen-bonding interactions, respectively. Complexes **1**, **2**, **6**, **7** and **9** possess a 2D layered structure, and the 2D frameworks of complexes **1**, **2** and **6** can be rationalized to be four-connected $\{4^4\cdot 6^2\}$ topological ***sql*** networks with the dinuclear units, while **9** shows a two dimensional six-connected $\{3^6\cdot 4^6\cdot 5^3\}$ topological ***hxl*** network containing $[Cd_4(OH)_2(H_2O)_2(NO_3)_2]$ cluster. Complex **3** bearing the 3D framework can be rationalized to be a new $\{3^{18}\cdot 4^{18}\cdot 5^9\}$ topological net with the stoichiometry (10-c). Complex **5** features the 3D topological ***tcj***/***hc*** structure of $\{3^6\cdot 4^6\cdot 5^3\}\{3^6\cdot 4^8\cdot 5^4\cdot 6^8\cdot 7^2\}$ with the stoichiometry (6-c)(8-c). Both complexes **3** and **5** contain 1D channels with the accessible solvent volume of 38.8% and 12.1%, respectively. Obviously, structural differences among those complexes are attributable to various coordination modes and flexible configurations of ligands, the different metal ions, pH values, temperature and counter anions, etc. Furthermore, the fluorescent emission and fluorescence lifetime of **1**–**9** have been investigated.

Introduction

Since last century, design and synthesis of metal−organic complexes have attracted tremendous interest for not only their attractive structures and topological networks[1] but also their potential applications in luminescence,[2] molecular magnetism,[3] chemical sensors,[4] gas adsorption,[5] conductivity,[6] catalysis,[7] proton conduction,[8] drug delivery,[9] embedding of nanoparticles,[10] and so on. Thanks to the constant efforts of the chemists, some achievements have been made in these areas.[11] However, obtaining predetermined structures and desired properties still pose tremendous scientific challenges, because there are so many factors influencing the construction of complexes, such as the coordination requirements of metal centers, solvent systems, temperatures, pH values and features of organic ligands, and so on.[12-15]

The tetrazole with the four nitrogen atoms of the functional group have an excellent coordination ability to act as either a multidentate ligand or a bridging building block in supramolecular assemblies.[16] Recently, nitrogen-rich tetrazoles, especially 5-substituted 1H-tetrazoles have attracted considerable interest due to their novel structural architectures and topologies, and potential applications in coordination chemistry, medicinal chemistry and materials science.[17-21] 5-Substituted tetrazolate group, possessing acidity close to carboxylate group, with four nitrogen atoms being able to exhibit versatile bridging or chelating modes, has been extensively used in medicinal, coordination and material chemistry.[22, 23]

Some new coordination polymers based on flexible bis(tetrazol-5-yl)alkanes ligands [e.g. 1,2-bis(tetrazol-5-yl)ethane, 1,3-bis(tetrazol-5-yl)propane, 1,5-bis(tetrazol-5-yl)pentane] generally exhibit intriguing structures and luminescent properties.[24] The CH_2 groups of those bis(tetrazol-5-yl)alkanes ligands substituted by some heteroatoms such as N, O atoms which perhaps induce changes of charge density, space, solubility and coordination modes, may bring on significant conversion in the types of framework structures and functionalities.[25] For example, a zeolite-like microporous metal−organic framework (MOF) with 24 nuclear zinc cages based on 1,5-bis(5-tetrazolo)-3-oxapentane, the middle CH_2 group of 1,5-bis(tetrazol-5-yl) pentane substituted by O atom, was synthesized and characterized.[26] Deng and his coworkers used NH group to substitute the middle CH_2 group of 1,3-bis(tetrazol-5-yl)propane, and obtained a 3D framework consisting of cyclic $[Cd_2(BTMA)_2]$ [BTMA=bis-(1*H*-tetrazol-5-ylmethyl)-amine] dimer subunits, possessing an 8-connected framework with $\{4^4\cdot6^{16}\cdot8^8\}$ topology through *situ* synthesis.[27]

With the above consideration, in order to investigate the influences of NH groups inserted in bis(tetrazol-5-yl)alkanes ligands on the structures and properties of their complexes, two structurally related ligands, bis-(1*H*-tetrazol-5-ylmethyl)-amine ($H_3\mathbf{L^1}$) and bis-(1*H*-tetrazol-5-ylethyl)-amine ($H_3\mathbf{L^2}$) (**Scheme 1**) were prepared, two new 0D complexes $Cd_2(H\mathbf{L^1})_2(H_2O)_4\cdot2H_2O$ (**4**), $Cd(H\mathbf{L^2})(H_2O)_3$ (**8**), and seven new coordination polymers, $[Zn(H\mathbf{L^1})(H_2O)]_n$ (**1**), $[Zn(H\mathbf{L^1})]_n$ (**2**), $[Cd_3(H\mathbf{L^1})_2Cl_2]_n$ (**3**), $\{[Cd_2(H\mathbf{L^1})_2]\cdot H_2O\}_n$ (**5**), $[Zn(H\mathbf{L^2})]_n$ (**6**), $[Zn_2(H\mathbf{L^2})N_3Cl]_n$ (**7**) and $[Cd_2(H\mathbf{L^2})(NO_3)(OH)(H_2O)]_n$ (**9**) based on $H_3\mathbf{L^1}$ and $H_3\mathbf{L^2}$ were successfully prepared and structurally characterized. Interestingly, these compounds exhibit various network architectures with a wide range from 0D to 3D networks. Furthermore, the fluorescent emission and fluorescence lifetime of the complexes **1**–**9** have been investigated and discussed.

(Insert Scheme 1)

Experimental Section

Materials and General Methods. All the other reagents used for the syntheses were commercially available and employed without further purification. The ligands $H_3\mathbf{L^1}$ and $H_3\mathbf{L^2}$ used in this work were synthesized according to the literature procedure.[28] Elemental analyses of C, H and N were determined with a Thermo Flash EA 1112-NCHS-O analyzer. IR spectra were measured on a Brucker Equinox 55 FT-IR spectrometer with KBr pellets in the range of 4000–400 cm^{-1}. NMR data were collected by an INOVA-400 NMR spectrometer and chemical shifts are reported in δ relative to TMS. Solid state luminescent spectra of ligands $H_3\mathbf{L^1}$, $H_3\mathbf{L^2}$ and complexes **1**-**9** were measured by Hitachi F-4500 Fluorescence Spectrophotometer with a Xe arc lamp as the light source and bandwidths of 2.5 nm at room temperature. Fluorescence lifetime data were acquired on Fluorolog-3 spectrofluorimeter equipped with nanoled as the light source. The X-ray powder diffraction (PXRD) was recorded on a Rigaku D/Max-2500 diffractometer at 40 kV, 100 mA for a Cu-target tube and a graphite monochromator.

Synthesis of complexes 1~9

$[Zn(HL^1)(H_2O)]_n$ (1)

A mixture of $ZnCl_2$ (244.5 mg, 1.8 mmol), $H_3\mathbf{L^1}$ (108.3 mg, 0.6 mmol), NaOH (23.9 mg, 0.6 mmol) in H_2O (10 mL) was stirred for 30 min at room temperature and then sealed in a 25 mL Teflon-lined autoclave at 140 °C for 24 hours. After the mixture was cooled to room temperature at a rate of 5 °C h^{-1}, colorless rod-like single crystals of **1** were obtained. Yield: 35% based on $H_3\mathbf{L^1}$. Anal. Calcd(%) for $C_4H_7N_9OZn$: C, 18.30; H, 2.69; N, 48.01. Found: C, 18.16; H, 2.53; N, 47.91. IR (KBr pellets, cm^{-1}): 3616 *m,* 3252 *s,* 1634 *m,* 1500 *m,* 1434 *s,* 1325 *m,* 1254 *m,* 1228 *m,* 1160 *w,* 1126 *s,* 1081 *s,* 1053 *w,* 1035 *w,* 1014 *s,* 915 *s,* 766 *w,* 698 *w.*

$[Zn(HL^1)]_n$ (2)

A mixture of $Zn(NO_3)_2{\cdot}6H_2O$ (178.5 mg, 0.6 mmol), $H_3\mathbf{L^1}$ (54.3 mg, 0.3 mmol), NaOH (12.0 mg, 0.3 mmol), and NaN_3 (19.5 mg, 0.3 mmol) in H_2O (7 mL) was stirred for 30 min at room temperature and then sealed in a 25 mL Teflon-lined autoclave at 130 °C for 72 hours. After the mixture was cooled to room temperature at a rate of 5 °C h^{-1}, colorless rod-like single crystals of **2** were obtained. Yield: 31% based on $H_3\mathbf{L^1}$. Anal. Calcd(%) for $C_4H_5N_9Zn$: C, 19.65; H, 2.06; N, 51.55. Found: C, 19.47; H, 2.13; N, 51.29. IR

(KBr pellets, cm^{-1}): 3633 *m*, 3579 *m*, 3429 *m,* 3298 *s*, 2963 *m*, 2928 *w*, 1594 *w*, 1511 *m*, 1495 *m*, 1456 *m*, 1439 *s*, 1420 *s*, 1345 *s*, 1276 *s*, 1248 *m*, 1230 *s*,1165 *m*, 1151 *w*, 1117 *s*, 1101 *s*, 1081 *s*, 1026 *m*, 987 *s*, 930 *w*, 881 *m*, 783 *w*, 739 *w*, 706 *m*, 685 *w*.

$[Cd_3(HL^1)_2Cl_2]_n$ (3)

A mixture of $CdCl_2·2.5H_2O$ (137.0 mg,0.6 mmol), $H_3\mathbf{L^1}$ (54.3 mg, 0.3 mmol), NaOH (12.0 mg, 0.3 mmol) in H_2O (7 mL) was stirred for 30 min at room temperature and then sealed in a 25 mL Teflon-lined autoclave at 140 °C for 48 hours. After the mixture was cooled to room temperature at a rate of 5 °C h^{-1}, colorless rod-like single crystals of **3** were obtained. Yield: 30% based on $H_3\mathbf{L^1}$. Anal. Calcd(%) for $C_8H_{10}N_{18}Cl_2Cd_3$: C, 12.53; H, 1.32; N, 32.90. Found: C, 12.28; H, 1.03; N, 32.47. IR (KBr pellets, cm^{-1}): 3422 *s*, 3265 *s*, 2918 *w*, 1627 *m*, 1498 *m*, 1441 *m*, 1428 *m*, 1342 *m*, 1232 *m*, 1230 *m*,1175 *m*, 1157 *m*, 1131 *m*, 1111 *m*, 1078 *w*, 1051 *w*, 1019 *m*, 912 *m*, 781 *w*, 750 *w*, 711 *w*, 692 *w*, 532 *m*, 446 *m*.

$Cd_2(HL^1)_2(H_2O)_4·2H_2O$ (4)

$Cd(CH_3COO)_2·2H_2O$ (26.7 mg, 0.1 mmol) and $H_3\mathbf{L^1}$ (18.1 mg, 0.1 mmol) was dissolved in H_2O (15 mL) and filtrated. Colorless rod-like single crystals were formed after several days with the evaporation of the solvent. Yield: 35% based on $H_3\mathbf{L^1}$. Anal. Calcd(%) for $C_8H_{22}N_{18}O_6Cd_2$: C, 13.90; H, 3.21; N, 36.48. Found: C, 13.78; H, 3.03; N, 36.77. IR (KBr pellets, cm^{-1}): 3245 *s*, 3153 *s*, 2930 *m*, 1682 *w*, 1596 *w*, 1489 *w*, 1466 *m*, 1429 *m*, 1359 *w*, 1237 *w*, 1210 *w*, 1159 *m*, 1136 *m*, 1120 *m*, 1089 *m*, 1057 *w*, 1031 *w*, 981 *m*, 950 *m*, 834 *m*, 754 *m*, 715 *m*, 689 *m*.

$\{[Cd_2(HL^1)_2]·H_2O\}_n$ (5)

A mixture of $CdCl_2·2.5H_2O$ (137.0 mg, 0.6 mmol), $H_3\mathbf{L^1}$ (54.3 mg, 0.3 mmol), and a drop of triethylamine (TEA) in H_2O (7 mL) was stirred for 30 min at room temperature and then sealed in a 25 mL Teflon-lined autoclave at 140 °C for 48 hours. After the mixture was cooled to room temperature at a rate of 5 °C h^{-1}, colorless rod-like single crystals of **5** were obtained. Yield: 34% based on $H_3\mathbf{L^1}$. Anal. Calcd(%) for $C_8H_{12}N_{18}OCd_2$: C, 15.98; H, 2.01; N, 41.94. Found: C, 15.71; H, 2.03; N, 41.47. IR (KBr pellets, cm^{-1}): 3428 *s*, 3230 *s*, 2874 *m*, 2824 *m*, 1626 *m*, 1493 *m*, 1410 *s*, 1346 *m*, 1246 *m*, 1175 *m*, 1142 *m*, 1080 *m*, 1018 *m*, 961 *w*, 891 *w*, 822 *w*, 790 *w*, 755 *w*, 715 *w*, 675 *w*.

$[Zn(HL^2)]_n$ (6)

A mixture of $Zn(BF_4)_2·6H_2O$ (138.8 mg, 0.4 mmol), iminodipropionitrile (24.6 mg, 0.2 mmol), and NaN_3 (19.5 mg, 0.3 mmol) in H_2O (7 mL) was stirred for 30 min at room temperature and then sealed in a 25 mL Teflon-lined autoclave at 160 °C for 72 hours. After the mixture was cooled to room temperature at a rate

of 5 °C h^{-1}, colorless block-like single crystals of **6** were obtained. Yield: 39% based on iminodipropionitrile. Anal. Calcd (%) for $C_6H_9N_9Zn$: C, 26.43; H, 3.33; N, 46.25. Found: C, 26.05; H, 3.34; N, 45.94. IR (KBr pellets, cm^{-1}): 3261 *s*, 2952 *m*, 2924 *m*, 2876 *m*, 2823 *w*, 2079 *w*, 1566 *w*, 1492 *s*, 1462 *m*, 1419 *s*, 1368 *m*, 1330 *m*, 1286 *m*, 1255 *m*, 1237 *m*, 1194 *w*, 1122 *m*, 1107 *s*, 1079 *m*, 1029 *w*, 980 *s*, 935 *w*, 883 *m*, 815 *m*, 739 *w*, 725 *m*, 671 *m*.

$[Zn_2(HL^2)N_3Cl]_n$ (7)

A mixture of $ZnCl_2$ (81.7 mg,0.6 mmol), iminodipropionitrile (24.6 mg, 0.2 mmol), and NaN_3 (19.5 mg, 0.3 mmol) in H_2O (5 mL) and CH_3CH_2OH (2.5 mL) was stirred for 30 min at room temperature and then sealed in a 25 mL Teflon-lined autoclave at 140 °C for 24 hours. After the mixture was cooled to room temperature at a rate of 5 °C h^{-1}, colorless rod-like single crystals of **7** were obtained. Yield: 30% based on iminodipropionitrile. Anal. Calcd(%) for $C_6H_{10}ClN_{12}Zn_2$: C, 17.30; H, 2.42; N, 40.36. Found: C, 17.07; H, 2.53; N, 40.94. IR (KBr pellets, cm^{-1}): 3359 *s*, 3277 *s*, 2994 *m*, 2960 *w*, 2316 *w*, 2144 *w*, 2083 *w*, 1683 *w*, 1618 *w*, 1594 *m*, 1485 *m*, 1439 *m*, 1431 *m*, 1406 *s*, 1322 *m*, 1302 *w*, 1275 *m*, 1420 *m*, 1183 *s*, 1114 *m*, 107 *s*, 1041 *w*, 1018 *w*, 855 *w*, 943 *w*, 911 *w*, 751 *w*, 652 *m*, 639 *m*.

$Cd(HL^2)(H_2O)_3$ (8)

$CdCl_2 \cdot 2.5H_2O$ (91.34 mg, 0.4 mmol) and $H_3\mathbf{L}^2$ (41.8 mg, 0.2 mmol) was dissolved in H_2O (10 mL) and then concentrated ammonium hydroxide (3 mL) was added to the mixture and filtrated. Colorless rod-like single crystals of **8** were formed after several days with the evaporation of the solvent. Yield: 33% based on $H_3\mathbf{L}^2$. Anal. Calcd(%) for $C_6H_{15}N_9O_3Cd$: C, 19.29; H, 4.05; N, 33.73. Found: C, 19.70; H, 4.21; N, 33.48. IR (KBr pellets, cm^{-1}): 3433 *s*, 3221 *s*, 2873 *m*, 2825 *m*, 2499 *w*, 1626 *m*, 1493 *m*, 1411 *s*, 1345 *m*, 1286 *w*, 1251 *m*, 1175 *m*, 1142 *m*, 1110 *m*, 1080 *m*, 1045 *w*, 961 *w*, 891 *w*, 822 *w*, 790 *w*, 755 *w*, 714 *w*, 675 *w*.

$[Cd_2(HL^2)(NO_3)(OH)(H_2O)]_n$ (9)

A mixture of $Cd(NO_3)_2 \cdot 4H_2O$ (123.4 mg, 0.4 mmol), one drop of concentrated ammonium hydroxide and $H_3\mathbf{L}^2$ (41.8 mg, 0.2 mmol) was dissolved in H_2O (3.5 mL) and CH_3CH_2OH (3.5 mL) and stirred for 30 min at room temperature and then sealed in a 25 mL Teflon-lined autoclave at 140 °C for 48 hours. After the mixture was cooled to room temperature at a rate of 5 °C h^{-1}, colorless rod-like single crystals of **9** were obtained. Yield: 31% based on $H_3\mathbf{L}^2$. Anal. Calcd(%) for $C_6H_{12}N_{10}O_5Cd_2$: C, 13.62; H, 2.29; N, 26.48. Found: C, 13.67; H, 2.33; N, 26.34. IR (KBr pellets, cm^{-1}): 3583 *m*, 3439 *m*, 3224 *s*, 3090 *m*, 2956 *m*, 2913 *m*, 2868 *m*, 2280 *w*, 1774 *w*, 1653 *w*, 1560 *w*, 1499 *m*, 1475 *m*, 1414 *s*, 1371 *s*, 1347 *s*, 1251 *m*, 1218 *w*, 1173 *m*, 1161 *m*, 1131 *m*, 1110 *w*, 1095 *w*, 983 *w*, 894 *w*, 827 *m*, 811 *m*, 763 *w*, 750 *w*, 679 *m*, 750 *m*.

X-ray Crystallography. The X-ray diffraction (XRD) data of complexs **1**-**9** were collected on a Bruker APEX II Smart CCD diffractometer at 296(2) K with Mo-Kα radiation (λ = 0.71073 Å) by *ω*-*φ*scan mode. Semi-empirical absorption corrections were applied to the data using SADABS program. The program SAINT[29] was used for integration of the diffraction profiles. The structures were solved by direct methods using the SHELXS program of the SHELXTL package and refined by full-matrix least-squares methods with SHELXL[30] Metal atoms in each complex were located from the E-maps and other non-hydrogen atoms were located in successive difference Fourier syntheses and refined with anisotropic thermal parameters on F^2. Hydrogen atoms of carbon were located at calculated positions and refined with fixed thermal parameters riding on their parent atoms. The crystallographic data for compounds **1**–**9** are listed in Table 1, and selected bond lengths and angles are given in Table S1 of Supplementary 1.

All crystal data file in CIF format was deposited in CCDC and reference numbers 1423982 for **1**, 1034433 for **3**, 1034430 for **6**, 1473508-1473513 (for complex **2, 4, 5**, **7**-**9**, respectively). This data can be obtained from the Cambridge Crystallographic Data Center, 12 Union Road, Cambridge CB2 1EZ, UK; Fax: +44 1223 336033; E-mail: deposit@ccdc.cam.ac.uk.

(Insert Table **1**)

Results and Discussion

Synthesis and General Characterization.

It is well-known that the selection or design of organic ligands containing appropriate coordination sites is crucial to construct fascinating coordination frameworks with intriguing different structures. Sharpless et al. reported a safe, convenient and environmentally friendly method to prepare 5-substituted-1*H*-tetrazole using organic cyano compounds and NaN_3 in the presence of Zn^{II} salts as catalysts in water.[28, 31]

Here we utilized NaN_3 to react with iminodiacetonitrile and iminodipropionitrile, respectively, and obtained two flexible bis(tetrazole) ligands $H_3\mathbf{L}^1$ and $H_3\mathbf{L}^1$, and the ligands $H_3\mathbf{L}^1$ and $H_3\mathbf{L}^2$ are potential not only bridging ligands but also chelating ligands with as many as nine nitrogen coordination sites. In this work, to better explore the synthetic factors impacting on the construction of complexes, two 0D complexes **4** and **8** were synthesized via slow evaporation at room temperature, and seven 2D or 3D coordination polymers **1**-**3**, **5**-**7** and **9** were prepared in a 25 mL Teflon-lined stainless steel autoclave under hydro(solvo)-thermal conditions (**Scheme 2**). This indicates that hydro(solvo)-thermal conditions are easier to form high dimensional coordination polymers. We obtained two different 2D frameworks of Zn(II) complexes, when using $ZnCl_2$ and $Zn(NO_3)_2{\cdot}6H_2O$ to react with ligand $H_3\mathbf{L}^1$, respectively, through

changing the solvent and temperature of hydro(solvo)-thermal conditions. Interestingly, although NaN_3 is not present in compound **2**, the final products did not present any crystallinity without NaN_3, which indicates that small ancillary bridging ligands like NaN_3 plays a critical role in the formation of **2**. Furthermore, the reaction systems of **3** and **5** are almost the same except that inorganic alkali NaOH and organic alkali TEA were utilized for their preparation, respectively, but the Cl^- anions participate in the construction of **3** rather than **5** and the size of channels is much bigger than that of **5**, thus forming two entirely different 3-D frameworks and topological structures. This suggests that different types of alkali have disparate effects on the constructions of MOFs. For compounds **6** and **7**, to the best of our knowledge, this is the first case of bis(2-cyanoethyl)amine as the initial reactant in situ hydro(solvo)-thermal synthesis of bis-(1*H*-tetrazol-5-ylethyl)-amine complexes. It is interesting that the **6** and **7** have different 2D network structures. Obviously, the structural difference of **6** and **7** is attributable to the difference of counter anions, temperature and solvent, the Cl^- anions and azido ions participating in coordinating in **7**.

In the FT-IR spectra of the synthetic products, the strong bands that appeared around 3400 cm^{-1} should be ascribed to the stretching vibrations of O-H or N-H, suggesting the presence of free or coordinated water molecule and the N-H in coordinated ligands. The peak at 2083 cm^{-1} for the asymmetric stretching of N_3^- for **7** confirms the existence of the azide anion in the compound, and in **9**, the absorption band appearing at 1371 cm^{-1} is characteristic of a coordinated NO_3^- ions. All complexes exhibit peaks in the 1400-1500 cm^{-1} region clearly confirmed the formation of the tetrazole groups.

(Insert Scheme 2)

Crystal Structures

$[Zn(HL^1)(H_2O)]_n$ (1) X-ray crystallographic analysis shows that **1** crystallizes in the monoclinic space group *P*2(1)*/c* and features a 2D layer structure, and compound **1** consists of one Zn(II) center, one water molecule and one organic ligand H**L**^{1}. As shown in **Fig. 1a**, each Zn(II) atom is six-coordinated by five nitrogen atoms (N2, N3, N4, N5, N7) from three independent ligands H**L**^{1} and one oxygen atom (O1W) from one coordinated water molecule. The six-coordinated Zn(II) atom displays a distorted octahedron coordination geometry and the equatorial plane is occupied by four nitrogen atoms (N3, N4, N5, N7) and Zn1 (the mean deviation from plane is 0.0521 Å), while the atoms N2 and O1W occupy axial positions with the N2–Zn–O1W bond angle of 167.8(3)°. The Zn–N bond lengths are measured in the range of 2.079(9)-2.240(9) Å, and the Zn–O bond length is 2.249(9) Å. Of these five Zn–N bonds, the length of the

bond between Zn and N3 from the middle imino group is longer than that of bonds among Zn and N from tetrazole rings. As shown in **Fig. 1b** and **1c**, in the 2D coordination layers, two Zn1 cations are connected by a pair of H**L**^{1} ligands to form a [Zn_2(H**L**^{1})$_2$] dimer with a Zn1···Zn1 length of 4.083(6) Å (Fig. **1b**), and two adjacent [Zn_2(H**L**^{1})$_2$] dimers are further linked by Zn1-H**L**^{1} coordination interactions. Besides, when the [Zn_2(H**L**^{1})$_2$] dimer is simplified into a four-connected node, a 2D four-connected {$4^4\cdot6^2$} topological ***sql*** network is obtained (**Fig. 1d**). Because of the flexibility and conformational freedom of torsional C–C/C–N bonds in the ligand, the two tetrazole rings in the same H**L**^{1} are significantly twisted from each other with a dihedral angle of 98.83°. As a result, the entire ligand isn't linear and exhibits an open V-shaped conformation. In **1**, each ligand H**L**^{1} exhibits a tridentate chelating and bridging mode, and adopts a μ_3-κN2, N3, N4: κN5: κN7 coordination mode to bridge three Zn(II) centers through N2, N3, N4, N5 and N7 (as illustrated in **Scheme 3a**). Simultaneously, the tetrazolate rings of H**L**^{1} show two coordination modes (modes II and III in **Scheme 4**) in **1**.

(Insert **Fig. 1**)

(Insert Scheme 3 and 4)

[Zn(HL^{1})]$_n$ (2) Single crystal X-ray diffraction structural analysis reveals that compound **2** crystallizes in space group *P*2(1)*/n* and features a 2D net built up by the dimeric unit [Zn_2(H**L**^{1})$_2$] (**Fig. 2b**), also resulting in a similar 2D four-connected {$4^4\cdot6^2$} topological ***sql*** network (**Fig. 2c**). As shown in **Fig. 2a**, compound **2** also includes an asymmetric unit consisting of one Zn(II) ion and one H**L**^{1} ligand. Each Zn(II) ion has a distorted trigonal bipyramid geometry [ZnN_5]. The five coordination positions are filled with N1, N6, N9, N2 and N5 from two different H**L**^{1} ligand, and the equatorial plane is occupied by three nitrogen atoms (N1, N6, N9) (the mean deviation of Zn from plane is 0.0521 Å), while N2 and N5 occupy axial positions with the N2–Zn–N5 bond angle of 171.08(3)°. The Zn–N5 bond distance is 2.546(3) Å, which is much bigger than the other analogues ranging from 1.993(3) to 2.109(3) Å. Furthermore, the closest Zn···Zn separation across the azole rings is 3.967(2) Å, which is shorter than that in **1**. The dihedral angle between two tetrazole rings in the same H**L**^{1} is 124.50°, which is bigger than that in **1**. In **2**, for both the whole ligands and tetrazolate rings linking three symmetry related Zn centers, they show the same coordination modes μ_3-κN1, N5, N9: κN2: κN6 as displayed in **1** (**Scheme 3a**).

(Insert **Fig. 2**)

[Cd$_3$(HL^{1})$_2$Cl$_2$]$_n$ (3) Crystal structure analysis of **3** indicates a 3D framework crystallize in the hexagonal system with space group *R*-3. In complex **3**, the asymmetric unit contains two crystallographically

independent Cd(II) centers that adopt different coordination environments, one H**L**[1] ligand and one μ_2-Cl^- anion. As illustrated in **Fig 3a**, Cd1 center is six-coordinated by six nitrogen atoms from four unique H**L**[1] ligands and one chlorine ion, completing a distorted monocapped octahedral geometry, and the Cd1–N bond lengths are measured in the range of 2.328(2)–2.807(2) Å, while Cd1–Cl bond length is 2.6140(8) Å. Considering the connection of the Cd1 centers, H**L**[1] ligand and Cl^- anion, the Cd1 centers are linked by the tetrazole groups (adopt a $\mu_{1,2}$ coordination mode, mode II in **Scheme 4**) of H**L**[1] ligands to form infinite one dimensional(1D) right-handed helical chains, with –Cd1-tetrazole-Cd1- helical chains extending along the b axis (as illustrated in **Fig. 3b**). The Cd2 center assumes slightly distorted octahedral coordination geometry [CdN_4Cl_2] (**Fig. 3c**). The two Cl^- anions occupy the apical positions with the Cl–Cd–Cl bond angle of 179.964(3)°, while the Cd2–Cl bond length is 2.6145(8) Å, and the other four atoms (N7, N7**h**, N8 and N8**h**) are seated in the equatorial sites with the Cd2–N bond distances being 2.321(2) and 2.311(2) Å, respectively. Considering the connection of the Cd2 center, H**L**[1] ligand and Cl^- anion, adjacent Cd2 centers are bridged by a pair of ligands H**L**[1] to give a 1D chain along the c-axis (**Fig. 3d**). The Cl^- anions adopt a μ_2 bridging mode linking Cd1 center and Cd2 center. In **3**, the tetrazolate rings of H**L**[1] adopt two types of coordination modes (modes V and VI in **Scheme 4**), and all the H**L**[1] ligands adopt a μ_6-κN1, N2, N3: κN5: κN6: κN7:κN8 bridging mode to link six cadmium ions (**Scheme 3c**). As a result, the structure of **3** is assembled into a 3-D network (**Fig. 3e**). It is interesting that 1-D channels in the 3-D framework can be observed along the *c* axis, and the channels' inner surface is decorated by Cl^- anions. Furthermore, the accessible solvent volume is 38.8% per unit cell volume as calculated by PLATON. It is noted that the structure of **3** contains a trinuclear [Cd_3Cl_2] subunit which is built by the interconnection among one Cd2 and two Cd1 cations and three Cl^- anions. From the topological point of view, each trinuclear [Cd_3Cl_2] unit can be considered as a 10-connected node. Thus, the overall structure of **3** can be simplified as a 3D 10-connected net with new $\{3^{18}\cdot4^{18}\cdot5^9\}$ topology (**Fig. 3f**).

(Insert **Fig. 3**)

$Cd_2(HL^1)_2(H_2O)_4\cdot2H_2O$ (4) The crystal data show that complex **4** crystallizes in the monoclinic system with *P*2(1)*/n* space group. There is one crystallographically-independent Cd(II) center, one coordinating H**L**[1] ligand, two coordinating water molecules and one lattice water molecule in the asymmetric unit. As exhibited in **Fig. 4**, complex **4** reveals a centrosymmetric dinuclear structure, and the Cd(II) center adopts a distorted octahedral coordination geometry [CdN_4O_2]. The Cd(II) center is six-coordinated to four nitrogen atoms[N1, N5, N9, N2] from two unique H**L**[1] ligands [Cd1–N bond lengths are observed in the range of

2.2871(19)–2.434(2) Å] and two oxygen atoms from water molecule [Cd1-O bond lengths are 2.303(2) and 2.327(2) Å, respectively]. In addition, the Cd(II) ion is approximately coplanar with these four equatorial nitrogen atoms with a mean deviation of 0.024 Å. In the crystal structure of **4**, the tetrazolate rings of H**L**^{1} ligand adopt two coordination modes (modes I and II in **Scheme 4**) with a dihedral angle of 179.12°, and all the H**L**^{1} ligands adopt a μ_2-κN1, N5, N9: κN2 bridging mode to link two cadmium atoms with the distance of 4.4880(3) Å (**Scheme 3b**). It should be pointed out that O3–H6W···N8, O1–H1W···O3 and O2–H4W···N3 intermolecular hydrogen-bonding interactions are observed between adjacent dinuclear structures. Thus the adjacent dinuclear $Cd_2(HL^1)_2(H_2O)_4\cdot 2H_2O$ molecules are arranged into a 1D chain by the intermolecular hydrogen-bonding interactions (see **Fig. S1a** of Supplementary 2). Additionally, the O1–H2W···N6 hydrogen-bonding interactions are observed between adjacent chains, such 1D chains were assembled by the hydrogen-bonding interactions between adjacent chains into an infinite 2D supramolecular sheet (**Fig. S1b** of Supplementary 2). At the same time, the infinite 2D supramolecular sheets are arranged into a three-dimensional supramolecular sheet (**Fig. S1c** of Supplementary 2) by the O3–H5W···N4 hydrogen-bonding interactions. In order to better understand the 3D supramolecular sheet, we take each dinuclear structure as a 14-connected node and the hydrogen-bonding as a linker, and thus, the 3D supramolecular sheet can be rationalized to be a uninodal $\{3^{36}\cdot 4^{48}\cdot 5^{7}\}$ topological ***bcu-x*** net with the stoichiometry (14-c) (**Fig. S1d** of Supplementary 2). The hydrogen-bonding geometry of **4** is listed in Table S**2** of Supplementary 1.

(Insert **Fig. 4**)

$\{[Cd_2(HL^1)_2]\cdot H_2O\}_n$ (5) Crystal structure determination indicates that complex **5** also displays a 3D framework in the monoclinic space group *C*2/*c*, and the asymmetric unit is composed of two crystallographically independent Cd(II) ions [Cd1 and Cd2], one noncoordinating water molecule and one H**L**^{1} ligand. The Cd1 center is located in distorted octahedral coordination geometry [CdN_6], which is six-coordinated by six nitrogen atoms from four unique H**L**^{1} ligands [Cd1–N bond lengths are measured in the range of 2.296(2)– 2.460(2) Å] (**Fig. 5a**), and the adjacent Cd1 centers are linked via two tetrazole rings from two ligands with the distance of 5.627(2) Å to generate a 1D chain (**Fig. 5b**). As exhibited in **Fig. 5c**, Cd2 is also six-coordinated in a octahedral geometry, which is bonded by six nitrogen atoms from six H**L**^{1} ligands, resulting in a [CdN_6] octahedron that exhibits Cd2–N bond distances in the range of 2.307(2)–2.413(2) Å. At the same time, all the Cd2 centers are assembled into an infinite 2D sheet through a pair of ligands to give rise to an infinite 2D sheet (**Fig. 5d**).

In the structure of **5**, there exist two coordination modes of tetrazolate rings in H**L**^{2} with a dihedral angle of 63.62°, one adopts $\mu_{1,3}$ (mode VII in **Scheme 4**) while the other adopts $\mu_{1,2,4}$ (mode IV in **Scheme 4**) coordination mode. It should be pointed out that all the H**L**^{1} ligands are equivalent, and adopt μ_5-κN1, N9: κN4: κN4: κN6: κN8 coordination mode to link two Cd1 and three Cd2 centers with the closest Cd1···Cd2 distance of 6.285(2) Å (**Scheme 3d**), thus connecting the above infinite 1D chain and 2D sheet into 3D framework with 1D channels (**Fig. 5e**). The accessible solvent volume is 12.1% per unit cell volume as calculated by PLATON. Meanwhile, from the topological point of view, Cd1 and Cd2 can be described as 6-connected and 8-connected nodes, respectively, and the H**L**^{1} ligands are regarded as linear linkers. Thus, the whole structure of **5** can be simplified as a 3D binodal (6, 8)-connected ***tcj***/***hc*** net with the Schlafli symbol being $\{3^6\cdot4^6\cdot5^3\}\{3^6\cdot4^8\cdot5^4\cdot6^8\cdot7^2\}$ (**Fig. 5f**).

(Insert **Fig. 5**)

[Zn(HL^{2})]$_n$ (6) Complex **6** is a 2D framework that crystallizes in monoclinic space group *P*2(1)*/n*, and the asymmetric unit consists of a Zn(II) center and one tetrazole ligand H**L**^{2}. The Zn^{II} center features a distorted trigonal bipyramid geometry, which is five-coordinated by five N atoms from three different H**L**^{2} ligands (**Fig**. **6a**). There exist two coordination modes of tetrazolate rings in H**L**^{2} (**Fig. 6a**) (namely $\mu_{1,4}$ (mode III in **Scheme 4**) and $\mu_{1,2}$ (mode II in **Scheme 4**)). The dihedral angle between two tetrazole rings in the same H**L**^{1} is 100.92°. The Zn–N bond distances fall in the range of 2.0287(18)–2.1914(19) Å, and the equatorial plane is occupied by three nitrogen atoms (N1, N6, N7). As for Zn1, the mean deviation from the plane is 0.0304 Å, while atoms N2 and N5 occupy axial positions with the N2–Zn–N5 bond angle of 173.09(7)°. Interestingly, the N1 and N2 atoms from the same tetrazole rings of two H**L**^{2} ligands bridge two Zn(II) centers to construct a cyclic [Zn$_2$(H**L**^{2})$_2$] dimmer subunit with the Zn1···Zn1 distance of 4.144(4) Å (**Fig. 6**b), which is further assembled into a 2D layer structure via the connection of the same ligands. When simplifying the units [Zn$_2$(H**L**^{2})$_2$] into a 4-connected node and taking the H**L**^{2} bridges as linear linkers, a similar 2D four connected $\{4^4\cdot6^2\}$ topological ***sql*** network was obtained, which is the same as compounds **1** and **2** (**Fig. 6c**). In **6**, all the H**L**^{1} ligands are equivalent, and adopt a μ_3-κN1, N5, N6: κN2: κN7 coordination mode linking three Zn centers (**Scheme 3f**).

(Insert **Fig. 6**)

[Zn$_2$(HL^{2})N$_3$Cl]$_n$ (7) The single-crystal structure analysis of **7** reveals that **7** also displays a 2D framework in orthorhombic space group *Pnma,* the asymmetric unit of which contains two crystallographically independent Zn(II) ions (Zn1 and Zn2), one H**L**^{2}, one N_3^- anion and one Cl^- anion. In the crystal structure

of 7, Zn1 and Zn2 are located in totally different coordination environments. The Zn1 ion adopts distorted octahedral coordination enviroment [ZnN_6], in which Zn1 is six-coordinated by four nitrogen atoms from four tetrazole rings of four H**L**^{2} ligands, two nitrogen atoms from two different azido ions in the axial positions (**Fig. 7a**). Moreover, the Zn1 ion is approximately coplanar with the equatorial plane defined by the above four nitrogen atoms of H**L**^{2} ligands and the mean deviation is 0.094 Å. It is interesting that all the Zn1 centers in these structures octahedral [ZnN_6] spheres are bonded by triply-bridged tetrazolate–N and azido–N to form the above 1D building block (**Fig. 7b**), and the 1D building block is further assembled into 2D framework by the bridging action of the H**L**^{2} ligands (**Fig. 7c**). In addition, Zn2 ion is surrounded by three nitrogen atoms from one H**L**^{2} ligand and one chlorine ion (**Fig. 7d**), and the *cis*-angles at central Zn2 ions fall in the range of 95.00(7)–116.55(7)°, which indicates that the tetrahedral geometries around Zn2 centers are slightly distorted. As shown in **Fig. 7d**, two H**L**^{2} ligands, two Zn1 and two Zn2 ions formed a five-membered loop. Besides, the Zn1···Zn2 distances are 6.1549(4) Å and 6.3239(4) ÅThe whole 2D framework of **7** is composed of the Zn2 centers, Cl^- anions and the 2D net of Zn1 (**Fig. 7b**). In **7**, The azido ions adopt a $\mu_{1,1}$ bridging coordination mode linking two Zn1 centers with the distance of 3.4755 Å, while all the tetrazolate rings just adopt a $\mu_{1,2,4}$ (mode IV in **Scheme 4**) coordination mode, and all the H**L**^{2} ligands are also equivalent, adopting a μ_5-κN3, N4, N3**y**: κN1: κN1**s**: κN5: κN5**s** coordination mode linking four Zn1 and one Zn2 centers (**Scheme 3g**).

(Insert **Fig. 7**)

Cd(HL^2)(H$_2$O)$_3$ (8) Complex **8** crystallizes in the *Cc* space group, and selected bond distances and bond angles are presented in Table 1. X-ray single-crystal diffraction analysis indicates that **1** is a mononuclear structure, and the central Cd(II) ion is surrounded by three coordinating water molecules and one ligand H**L**^{2} in a distorted octahedral fashion N_3O, as shown in **Fig. 8**. The ligand H**L**^{2} adopts one tridentate a chelate coordinate fashion (**Scheme 3e**) by using two nitrogen atoms from the seperate tetrazole rings and the other nitrogen atom from the middle imino group in the H**L**^{2} to bond to the central Cd(II) ion (see **Fig. 8**), while the tetrazolate rings in H**L**^{2} ligand adopt mode I coordinate fashion with a dihedral angel of 169.80° (**Scheme 4**). Furthermore, the Cd–N bond lengths are measured in the range of 2.242(2)- 2.374(2) Å, and the Cd–O bond lengths are measured in the range of 2.316(3)- 2.472(2) Å. In addition, the hydrogen bonding interactions (O(3)– H(5W)···N(3) (O(3)···N(3) = 2.997(4) Å) and O(2)– H(3W)···N(6) (O(2)···N(6) = 2.777(4) Å)) are observed between adjacent molecules. Therefore, such structure units are further assembled into an infinite 1-D chain by the O–H···N hydrogen bonding interactions between

adjacent molecules (**Fig. S2a** of Supplementary 2). It should be pointed out that the hydrogen bonding interactions (O(2)– H(4W)···N(4) (O(2)···N(4) = 2.805(3) Å) and O(3)– H(6W)···N(7) (O(3)···N(7) = 2.984(4)) are observed between adjacent 1-D chains, so a two-dimensional framework (**Fig. S2b** of Supplementary 2) is formed in the complex by O–H···N hydrogen-bonding interactions. The hydrogen-bonding geometry of **8** is listed in Table S**2** of Supplementary 1.

(Insert **Fig. 8**)

$[Cd_2(HL^2)(NO_3)(OH)(H_2O)]_n$ (9) As revealed by single-crystal X-ray diffractions, the compound **9** crystallizes in the monoclinic space group *P*21/*c* as a 2D coordination polymer (**Fig. 9f**). The asymmetric unit of **9** contains two crystallographically independent Cd(II) ions, one ligand H**L**^{2}, one μ_3-OH^- anion, one nitrate ion and one coordinating water molecule. The two unique cadmium ions, both Cd1 and Cd2, have a distorted octahedral coordination geometry: Cd1 ion is coordinated by three nitrogen atoms from three different H**L**^{2} ligands, two μ_3-OH^- anion and one oxygen of nitrate ion (**Fig. 9a**); Cd2 center is surrounded by four nitrogen donors of two different H**L**^{2} ligands, one μ_3-OH^- anion and one water molecule (**Fig. 9c**). The Cd-N bond lengths vary from 2.2859(16) to 2.5047(16) Å, and Cd-O bond lengths range from 2.2465(13) to 2.526(15) Å. Two adjacent Cd1 centers are joint together to form dinuclear units Cd_2O_2 by two μ_3-OH^- anions with the distance of 13.486(2) Å, which are further bridged by a pair of tetrazoles from two H**L**^{2} ligands to generate a 2D network (**Fig. 9b**). The Cd2 centers are connected by the tetrazole groups of H**L**^{2} ligands to form infinite one dimensional right-handed helical chains, with -Cd2-tetrazole-Cd2- helical chains extending along the b axis (as illustrated in **Fig. 9d**). In **9**, two coordination modes $\mu_{1,2,4}$ (mode IV in **Scheme 4**) and $\mu_{1,2,3}$ (mode V in **Scheme 4**) are exhibited, and all the H**L**^{2} ligands are equivalent with a μ_5-κN1, N5, N9: κN3: κN4: κN7: κN8 coordination mode linking three Cd1 and two Cd2 centers (**Scheme 3h**). Interestingly, two Cd1 centers and two Cd2 centers are bridged via two μ_3-OH^- anions to generate a $[Cd_4(OH)_2(H_2O)_2(NO_3)_2]$ cluster with the Cd1···Cd2 distances of 3.6653(3) Å and 4.1550(3) Å (**Fig. 9e**). From this point of view, the 2D structure can be seen as being constructed by the clusters and the tetrazole groups, and each cluster is connected with other six clusters by four different tetrazole groups. To get a better insight into the structure of complex **9**, we used the TOPOS software to conduct topological analysis of the 2D framework. We take each $[Cd_4(OH)_2(H_2O)_2(NO_3)_2]$ cluster as a six-connected node and each tetrazole group as a linear connector (as shown in **Fig. 9g**). Consequently, a two dimensional six-connected topological ***hxl*** network with the point (Schläfli) symbol $\{3^6\cdot4^6\cdot5^3\}$ is formed as shown in **Fig. 9g**.

(Insert **Fig. 9**)

Effect of the flexible bistetrazole ligand on the architectures of MOFs

In this work, two flexible ligands that contain nine nitrogen coordination sites are selected to react with diverse Zn(II)/Cd(II) ions, which is aimed at observing how the ligands are adapted to fit in the environment of metal ions. On the one hand, because of the flexibility and conformational freedom of torsional $–CH_2–NH–CH_2–$/$–(CH_2)_2–NH–(CH_2)_2–$ bonds in the ligands, the tetrazoles in the same ligands H**L**^{1} and H**L**^{2} exhibit dihedral angles in the range of 63.62–179.12° and 100.92–169.80°, respectively, thus causing the V-shaped ligands displaying different open angle. It is a remarkable fact that the entire H**L**^{1} ligand except the H atoms and the middle NH group in **4** are nearly located in the same plane, so is the H**L**^{2} ligand in **8**, which indicates that the H**L**^{1} are likely to present the expected flexibility in the construction of high dimensional frameworks and exhibit the rigidity during the formation of complexes with 0D structures.

On the one hand, both H**L**^{1} and H**L**^{2} ligands exhibit diverse multidentate chelating and coordination modes: coordination mode **a** for **1** and **2**, coordination mode **c** for **3**, coordination mode **b** for **4**, coordination mode **d** for **5**, coordination mode **f** for **6**, coordination mode **g** for **7**, coordination mode **e** for **8**, and coordination mode **h** for **9**. Besides, comparing the structure of complexes **1** and **2**, the H**L**^{1} ligands present the same bridging and chelating modes, but their spacers exhibit different bending and rotating ability, which results in different non-bonding Zn···Zn distances via a pair of tetrazoles. Moreover, in complex **3**, trinuclear $[Cd_3Cl_2]$ subunits are bridged by the H**L**^{1} ligand to give a 3D framework with the new 10-connected topological net. In complex **4**, the centrosymmetric dinuclear $Cd_2(H\mathbf{L}^{1})_2(H_2O)_4\cdot 2H_2O$ molecules are linked into a 3D supramolecular sheet via hydrogen-bonding interactions among the ligands and water molecules, which possesses topological ***bcu-x*** structure. In complex **5**, Cd1 and Cd2 centers are bridged into infinite 1D chains and 2D sheet, which are further assembled into a 3D framework with (6, 8)-connected topological ***tcj***/***hc*** net. Besides, there exist the other two different topological structures: a 2D 4-connected topological network ***sql*** for **1**, **2** and **6**, a 2D 6-connected topological network ***hxl*** for **9**.

PXRD measurement and thermal stabilities

To confirm the mass identities and phase purity of **1**–**9**, X-ray powder diffraction (PXRD) experiments were carried out for complexes **1**–**9**, and the experimental and simulated powder X-ray diffraction (PXRD) patterns of the corresponding complexes are shown in **Fig. S3** of Supplementary 2. Although the

experimental patterns have a few unindexed diffraction lines and some are slightly broadened in comparison with those simulated from the single crystal modes. It still can be considered favorably that the bulk synthesized materials and the as-grown crystals are homogeneous for **1**-**9**.

Complexes **1**–**9** are air stable and can retain their crystalline integrity under ambient conditions for a long time. TGA data were obtained for **1**–**9** in a flowing Ar environment from 30–700 °C at a heating rate of 10 °C min^{-1}. As shown in **Fig. S4** of Supplementary 2. TG curve of **1** exhibits a plateau before 344 °C and above this temperature, the framework starts to decompose rapidly. Complex **2** is stable and begins to collapse sharply after 330 °C. For complex **3**, the weight loss starts at about 322 °C. Above 322 °C, the framework decomposes swiftly. Upon heating, a two-step weight loss process was observed for **4** and **5**. The first weight loss of 15.27% from 74 °C to 146 °C (for **4**), 2.73% from 81 °C to 91 °C (for **5**), corresponds to the loss of noncoordinating or coordinating water molecules (calcd. 15.64% for **4**, 2.99% for **5**, respectively). The second weight losses are exhibited from 320 °C (for **4**) and 337 °C (for **5**), which can be attributed to the decomposing of the organic ligands. TG curves of **6** and **7** exhibit a good resemblance with **1**, and exhibits a plateau before 331°C (for **6**) and 315 °C (for **7**). Above the mentioned temperature, a rapid weight loss is observed due to the collapse of frameworks. **8** and **9** possess similar thermal stabilities, expressing two-step weight losses. Upon heating, the first weight losses of 14.21% from 69 °C to 160 °C (for **8**) and 3.68% from 100 °C to 160 °C (for **9**) corresponds to the loss of noncoordinating or coordinating water molecules or lattice water molecules (calcd. 14.46% and 3.40%, for **8** and **9**, respectively). Upon further heating, the second weight losses due to the decomposing of the organic ligands are exhibited from 310 °C (for **8**) and 300 °C (for **9**), respectively.

Photoluminescence properties

It is known that many d^{10} metal compounds exhibit luminescent properties.[32] The coordination compounds with the rational selection and design of conjugated organic spacers and metal centers can be efficient for obtaining new luminescence materials.[33] To investigate the luminescent properties of complexes **1**-**9**, the solid-state photoluminescence properties of complexes **1**–**9** as well as the ligands $H_3\mathbf{L}^1$ and $H_3\mathbf{L}^2$ were investigated at ambient temperature under the same experimental conditions and their emission spectra are given in **Fig. 8**. The free ligand $H_3\mathbf{L}^1$ exhibits blue fluorescent emission band at 417 nm upon excitation at 340 nm, which can be assigned to ligand-centered electronic transitions, that is, the $n \rightarrow \pi^*$ or $\pi \rightarrow \pi^*$ transition in nature according to the reported literature.[34] Upon excitation with 340 nm light, complexes **1**-**5**

display fluorescent emission bands at 426, 434, 421, 420 and 420 nm, respectively. The ligand $H_3\mathbf{L}^2$ exhibits blue fluorescent emission band at 422 nm upon excitation at 340 nm, and complexes **6-9** display fluorescent emission bands at 423, 420, 423 and 420 nm, respectively. These results reveal that the peaks of the emission spectra for **1-9** are very close to that of the corresponding free ligand $H_3\mathbf{L}^1$ and $H_3\mathbf{L}^2$, respectively, which can probably be attributed to the intraligand fluorescence originating from ligand-centered emission.[35]

All the fluorescence lifetime measurements for $H_3\mathbf{L}^1$, $H_3\mathbf{L}^2$ and **1-9** were performed with excitation at 340 nm and corresponding emission band. And all the decay curves are well fitted into a triexpotential function: $I_t = I_0 + A_1\exp(-t/\tau_1) + A_2\exp(-t/\tau_2) + A_3\exp(-t/\tau_3)$, where τ_1 ,τ_2 and τ_3 are defined as the fluorescence lifetimes (summarized in **Table S3**), while the average fluorescence lifetime were found to be 2.57 ns (for $H_3\mathbf{L}^1$), 3.03 ns (for $H_3\mathbf{L}^2$), 3.08 ns (for **1**), 3.91 ns (for **2**), 3.63 nm (for **3**), 3.07 ns (for **4**), 3.22 ns (for **5**), 3.19 ns (for **6**), 2.62 ns (for **7**), 2.50 ns (for **8**) and 2.01 ns (for **9**), respectively (**Fig. S5** of Supplementary 2). Although there is a remarkable difference among the structures of ligands and relevant complexes, their fluorecence lifetimes are similar. The above result indicates the lifetime of $H_3\mathbf{L}^1$ ligand is slightly shorter than that of relevant complexes, while it is reverse for $H_3\mathbf{L}^2$ ligand and related complexes. In addition, it is apparent that complexes **3** and **5** exhibit longer lifetimes, which are presumably facilitated by the diverse porosity and intertetrazole coupling in their structures. And the overall lifetimes of **1-9** are in the range of nanoseconds probably due to the flexibility of structures.[36]

(Insert **Fig. 10**)

Conclusion

In summary, two 0D complexes, seven 2D and 3D metal–organic coordination polymers based on zinc and cadmium metal cations with two structurally related flexible bis(tetrazole) ligands ($H_3\mathbf{L}^1$ and $H_3\mathbf{L}^2$) were obtained. All the compounds exhibit diverse intriguing structures: complexes **4** and **8** represent 0D structure, complexes **1**, **2, 6, 7** and **9** possess 2D layered structures constructed from infinite organic chains, and the 2D frameworks of complexes **1**, **2** and **6** can be rationalized to be a topological ***sql*** network; complex **9** shows a two dimensional six-connected topological ***hxl*** network containing $[Cd_4(OH)_2(H_2O)_2(NO_3)_2]$ cluster as secondary building unit; complex **3** with the 3D supramolecular sheet can be rationalized to be a uninodal $\{3^{18}\cdot4^{18}\cdot5^9\}$; complex **5** features the 3D topology structure of ***tcj***/***hc*** net. Besides, both complexes **3** and **5** exhibit 1D channels with the accessible solvent volume of 38.8% and 12.1%, respectively. In this work, the tetrazolate groups show seven different coordination modes (see **Scheme 4**), while both ligand

$H_3\mathbf{L}^1$ and $H_3\mathbf{L}^2$ exhibit diverse conformation and coordination modes (see **Scheme 3**). It is noteworthy that tuning the synthesis conditions, either changing the pH or temperature and selecting counter anions and metal ions is a key step in the formation of coordination polymers with tetrazolate ligands. At the same time, the variation of the ligand spacer of the flexible ligands as well as the reaction conditions lead to the construction of complexes with different structures. Additionly, the luminescent properties of compounds **1**-**9** indicate that they may be potential candidates for luminescent materials. In short, this study provides diverse approaches to construct new functional material.

Acknowledgements

This work was financially supported by the National Natural Science Foundation of China (No. 21361026).

References

1 (a) X. Q. Zhang, Y. F. Gao, H. T. Liu and Z. L. Liu, *CrystEngComm*, 2015, **17**, 6037; (b) H. Hahm, S. Kim, H. Ha, S. Jung, Y. Kim, M. Yoon and M. Kim, *CrystEngComm*, 2015, **17**, 8418; (c) J. He, M. Zeller, A. D. Hunter and Z. Xu, *CrystEngComm*, 2015, **17**, 9254; (d) H. L. Nguyen, F. Gandara, H. Furukawa, T. L. Doan, K. E. Cordova and O. M. Yaghi, *J. Am. Chem. Soc.*, 2016, **138**, 4330.

2 (a) X. S. Wu, J. Liang, X. L. Hu, X. L. Wang, B. Q. Song, Y. Q. Jiao and Z. M. Su, *Cryst. Growth Des.*, 2015, **15**, 4311; (b) B. Mohapatra and S. Verma, *Cryst. Growth Des.,* 2016, **16**, 696; (c) B. Kaustuv, R. Sandipan, K. Moumita and B. Kumar, *Cryst. Growth Des.*, 2015, **15**, 5604; (d) C. Wang, F. Xing, Y. L. Bai, Y. Zhao, M. X. Li and S. Zhu, *Cryst. Growth Des.*, 2016, **16**, 2277; (e) D. Singh and C. M. Nagaraja, *Cryst. Growth Des.*, 2015, **15**, 3356; (f) X. C. Shan, F. L. Jiang, D. Q. Yuan, M. Y. Wu, S. Q. Zhang and M. C. Hong, *Dalton Trans.*, 2012, **41**, 9411.

3 (a) S. D. Han, S. J. Liu, Q. L. Wang, X. H. Miao, T. L. Hu and X. H. Bu, *Cryst. Growth Des.*, 2015, **15**, 2253; (b) J. Yang, X. B. Liu, X. Q. Wang, F. N. Dai, Y. Zhou, B. Dong, L. L. Zhang, Y. R. Liu and D. F. Sun, *Cryst. Growth Des.*, 2015, **15**, 4198; (c) D. L. Reger, A. Leitner and M. D. Smith, *Cryst. Growth Des.*, 2015, **15**, 5637; (d) J. P. Zhao, Q. Yang, Z. Y. Liu, R. Zhao, B. W. Hu, M. Du, Z. Chang and X. H. Bu, *Chem. Commun.*, 2012, **48**, 6568.

4 (a) A. B. Nowakowski, J. W. Meeusen, H. Menden, H. Tomasiewicz and D. H. Petering, *Inorg. Chem.*, 2015, **54**, 11637; (b) F. Jones, *CrystEngComm*, 2012, **14**, 8374; (c) L. Guang and J. T. Hupp, *J. Am. Chem. Soc.*, 2010, **132**, 7832; (d) L. G. Beauvais, M. P. S. And and J. R. Long, *J. Am. Chem. Soc.*, 2000, **122**, 2763.

5 (a) F. L. Li, H. X. Li and J. P. Lang, *CrystEngComm*, 2016, **18**, 1760; (b) F. L. Hu, Y. X. Shi, H. H.

Chen and J. P. Lang, *Dalton Trans.*, 2015, **44**, 18795; (c) M. V. Chumillas, N. Marino, I. Sorribes, C. Vicent, F. Lloret and M. Julve, *CrystEngComm*, 2010, **12**, 122; (d) X. J. Li, F. L. Jiang, M. Y. Wu, L. Chen, J. J. Qian, K. Zhou, D. Q. Yuan and M. C. Hong, *Inorg. Chem.*, 2014, **53**, 1032.

6 (a) X. J. Li, X. F. Sun, X. X. Li, Z. H. Fu, Y. Q. Su and G. Xu, *Cryst. Growth Des.*, 2015, **15**, 4543; (b) F. Yang, H. L. Huang, X. Y. Wang, F. Li, Y. H. Gong, C. L. Zhong and J. R. Li, *Cryst. Growth Des.*, 2015, **15**, 5827; (c) J. M. Taylor, T. Komatsu, S. Dekura, K. Otsubo, M. Takata and H. Kitagawa, *J. Am. Chem. Soc.*, 2015, **137**, 11498; (d) L. E. Darago, M. L. Aubrey, C. J. Yu, M. I. Gonzalez and J. R. Long, *J. Am. Chem. Soc.*, 2015, **137**, 15703.

7 (a) A. Karmakar, G. M. D. M. Rúbio, M. F. C. Guedes da Silva, S. Hazra and A. J. L. Pombeiro, *Cryst. Growth Des.*, 2015, **15**, 4185; (b) I. Luz, F. X. L. I. Xamena and A. Corma, *J. Catal.*, 2010, **276**, 134; (c) A. Dhakshinamoorthy, M. Alvaro and H. Garcia, *Adv. Synth. Catal.*, 2011, **352**, 3022; (d) R. Fernandez, V. Enrique, G. Domingos, Mariana, J. Alcañiz, Jana, Gascon, Jorge, Kapteijn and Freek, *Appl. Catal., A*, 2011, **391**, 261; (e) F. X. L. I. Xamena, A. Abad, A. Corma and H. Garcia, *J. Catal.*, 2007, **250**, 294.

8 (a) R. Karthik and S. Natarajan, *Cryst. Growth Des.*, 2016, **16**, 2239; (b) T. Kundu, S. C. Sahoo and R. Banerjee, *Chem. Commun.*, 2012, **48**, 4998; (c) M. Sadakiyo, H. Okawa, A. Shigematsu, M. Ohba, T. Yamada and H. Kitagawa, *J. Am. Chem. Soc.*, 2012, **134**, 5472; (d) G. Maarten G, J. A. Jana, R. F. Enrique V, Gu. K. B. Sai Sankar, S. Eli; V. B. Herman, G. Jorge; K. Freek, *J. Catal.*, 2011, **281**, 177; (e) J. Stankiewicz, M. Tomás, I. T. Dobrinovitch, E. Forcénvázquez and L. R. Falvello, *Chem. Mater.*, 2014, **26**, 6.

9 (a) J. Q. Liu, X. F. Li, C. Y. Gu, J. C. S. Da Silva, A. L. Barros, S. Alves-Jr, B. H. Li, F. Ren, S. R. Batten, A. Thereza, *Dalton Trans.,* 2015, **44**, 19370. (b) L. Wang, Y. Z. Han, X. Feng, J. W. Zhou, P. F. Qi and B. Wang, *Coord. Chem. Rev.*, 2016, **307**, 361.

10 (a) M. Giménez Marqués, T. Hidalgo, C. Serre and P. Horcajada, *Coord. Chem. Rev.*, 2016, **307**, 342; (b) Z. G. Gu, H. Fu, T. Neumann, Z. X. Xu, W. Q. Fu, W. Wenzel, L. Zhang, J. Zhang and C. Wöll, *Acs Nano.*, 2016, **10**, 977; (c) Y. Fu, Z. Zhang, X. Yang, Y. Q. Gan, W. Chen, *RSC Adv.*, 2015, **5**, 86941.

11 (a) B. Bhattacharya and D. Ghoshal, *CrystEngComm*, 2015, **17**, 8388; (b) G. Nandi, R. Thakuria, H. M. Titi, R. Patra and I. Goldberg, *CrystEngComm*, 2014, **16**, 5244; (c) Z. Su, K. Cai, J. Fan, S. S. Chen, M. S. Chen and W. Y. Sun, *CrystEngComm*, 2010, **12**, 100; (d) J. W. Sun, M. T. Li, J. Q. Sha, P. F. Yan, C. Wang, S. X. Li and Y. Pan, *CrystEngComm*, 2013, **15**, 10584; (e) X. Pantelis, S. Ioannis, K. Emmanuel, G. E. Froudakis and P. N. Trikalitis, *Inorg. Chem.*, 2014, **53**, 679.

12 (a) A. Buragohain, M. Yousufuddin, M. Sarma and S. Biswas, *Cryst. Growth Des.*, 2016, **16**, 842; (b) D. Sun, Y. H. Li, S. T. Wu, H. J. Hao, F. J. Liu, R. B. Huang and L. S. Zheng, *CrystEngComm*, 2011, **13**, 7311.

13 (a) X. Y. Wu, P. Dong, R. Yu, Q. K. Zhang, X. Kuang, S. C. Chen, Q. P. Lin and C. Z. Lu, *CrystEngComm*, 2011, **13**, 3686. (b) C. Eugenio, G. M. Monica, M. E. Guillermo, R. Fernando, V. Y. Inigo J, *J. Am. Chem. Soc.*, 2013, **135**, 15986.

14 (a) J. Cordes, P. R. D. Murray, A. J. P. White and A. G. M. Barrett, *Org. Lett.*, 2013, **15**, 4992; (b) Y. X. Shi, F. L. Hu, W. H. Zhang and J. P. Lang, *CrystEngComm*, 2015, **17**, 9404.

15 (a) W. Chen, J. Chu, I. Mutikainen, J. Reedijk, U. Turpeinen and Y. F. Song, *CrystEngComm*, 2011, **13**, 7299; (b) L. N. Zhang, X. L. Sun, C. X. Du and H. W. Hou, *Polyhedron*, 2014, **72**, 90.

16 B. Liu, Y. C. Qiu, G. Peng and H. Deng, *CrystEngComm,* 2010, **12**, 270.

17 (a) J. Pan, F. L. Jiang, M. Y. Wu, L. Chen, X. Y. Wan, Y. Yang, H. Xue, M. X. Yu and M. C. Hong, *Inorg. Chem. Commun.*, 2015, **56**, 129; (b) O. A. Bondar, L. V. Lukashuk, A. B. Lysenko, H. Krautscheid, E. B. Rusanov, A. N. Chernega and K. V. Domasevitch, *CrystEngComm*, 2008, **10**, 1216; (c) G. E. Kostakis, A. Mavrandonakis, G. Abbas, W. Klopper, D. Schooss, S. Lebedkin, Y. Lan and A. K. Powell, *CrystEngComm*, 2009, **11**, 2480.

18 (a) A. Rodríguez Diéguez, A. Salinas Castillo, A. Sironi, J. M. Seco and E. Colacio, *CrystEngComm*, 2010, **12**, 1876; (b) Y. B. Xie, L. Gan, E. Carolina Sañudo, H. Y. Zheng, J. P. Zhao, M. J. Zhao, B. Wang and J. R. Li, *CrystEngComm*, 2015, **17**, 4136; (c) X. Wang, A. X. Tian and X. L. Wang, *RSC Adv.*, 2015, **5**, 41155; (d) T. Zhao, K. Kurpiewska, J. Kalinowska Tluscik, E. Herdtweck and A. Domling, *Chem. Eur. J.*, 2016, **22**, 3009.

19 (a) T. Hosseinnejad and M. Dinyari, *Comput. Theor. Chem.,* 2015, **1071**, 53; (b) H. Naeimi and F. Kiani, *Ultrason. Sonochem.*, 2015, **27**, 408; (c) H. Gerhards, A. Krest, P. J. Eulgem, D. Naumann, D. Rokitta, M. Valldor and A. Klein, *Polyhedron*, 2015, **100**, 271.

20 (a) C. A. Zificsak and D. J. Hlasta, *Tetrahedron*, 2004, **60**, 8991; (b) P. Naumov and P. K. Bharadwaj, *CrystEngComm*, 2015, **17**, 8775.

21 (a) S. Nag and S. Batra, *Tetrahedron*, 2011, **67**, 8959; (b) H. R Jason, *Biorg. Med. Chem.*, 2002, **10**, 3379.

22 (a) I. Boldog, K. Domasevitch, J. K. Maclaren, C. Heering, G. Makhloufi and C. Janiak, *CrystEngComm*, 2014, **16**, 148; (b) R. T. Dong, X. L. Chen, Q. H. Li, M. Y. Hu, L. F. Huang, C. W. Li,

M. Y. Shen and H. Deng, *CrystEngComm*, 2015, **17**, 1305; (c) S. Zhao, J. Y. Dai, M. Hu, C. Liu, R. Meng, X. Y. Liu, C. Wang and T. P. Luo, *Chem. Commun.*, 2016, **52**, 4702.

23 (a) Y. Xiao, S. H. Wang, F. K. Zheng, M. F. Wu, J. Xu, Z. F. Liu, J. Chen, R. Li and G. C. Guo, *CrystEngComm*, 2016, **18**, 721; (b) N. Rezaee, A. Ahmadi and M. Z. Kassaee, *RSC Adv.*, 2016, **6**, 13224; (c) H. P. Fang, C. C. Fu, C. K. Tai, K. H. Chang, R. H. Yang, M. J. Wu, H. C. Chen, C. J. Li, S. Q. Huang, W. H. Lien, C. H. Chen, C. H. Hsieh, B. C. Wang, S. F. Cheung and P. S. Pan, *RSC Adv.*, 2016, **6**, 30362; (d) M. F. Wu, T. T. Shen, S. He, K. Q. Wu, S. H. Wang, Z. F. Liu, F. K. Zheng, G. C. Guo, *CrystEngComm*, 2015, **17**, 7473; (e) Z. F. Liu, M. F. Wu, S. H. Wang, F. K. Zheng, G. E. Wang, J. Chen, Y. Xiao, A. Q. Wu, G. C. Guo, J. S. Huang, *J. Mater. Chem. C.*, 2013, **1**, 4634.

24 (a) J. Y. Sun, L. Wang, D. J. Zhang, D. Li, Y. Cao, L. Y. Zhang, S. L. Zeng, G. S. Pang, Y. Fan, J. N. Xu and T. Y. Song, *CrystEngComm*, 2013, **15**, 3402; (b) I. Boldog, K. V. Domasevitch, I. A. Baburin, H. Ott, B. Gil Hernández, J. Sanchiz and C. Janiak, *CrystEngcomm*, 2013, **15**, 1235; (c) S. Goswami, S. Sanda and S. Konar, *CrystEngComm*, 2014, **16**, 369.

25 (a) Q. X. Han, B. Qi, W. M. Ren, C. He, J. Y. Niu, C. Y. Duan, *Nat. Commun.,* 2015, **6**, 10007; (b) I. Boldog, K. V. Domasevitch, J. Sanchiz, P. Mayer and C. Janiak, *Dalton Trans.*, 2014, **43**, 12590; (c) C. Huang, J. Wu, C. J. Song, R. Ding, Y. Qiao, H. W. Hou, J. B. Chang and Y. T. Fan, *Chem. Commun.*, 2015, **51**, 10353; (d) X. L. Tong, D. Z. Wang, T. L. Hu, W. C. Song, Y. Tao and X. H. Bu, *Cryst. Growth Des.*, 2009, **9**, 2280.

26 P. Cui, Y. G. Ma, H. H. Li, B. Zhao, J. R. Li, P. Cheng, P. B. Balbuena and H. C. Zhou, *J. Am. Chem. Soc.*, 2012, **134**, 18892.

27 Z. Y. Ma, L. X. Chen, L. F. Huang, Q. H. Li, M. Y. Hu, M. Y. Shen, C. W. Li and H. Deng, *CrystEngcomm*, 2015, **17**, 5814.

28 (a) H. Zhao, Q. Ye, Q. Wu, Y. M. Song, Y. J. Liu and R. G. Xiong, *Z. Anorg. Allg. Chem*., 2004, **630**, 1367; (b) Z. P. Demko, K. B. Sharpless, *J. Org. Chem*., 2001, **66**, 7945; (c) S. Fürmeier, O. M. Jürgen, *Eur. J. Org. Chem*., 2003, **5**, 885.

29 Bruker AXS, SAINT Software Reference Manual, Madison, WI, 1998.

30 G. M. Sheldrick, *Acta Crystallogr. Sect. A: Found. Crystallogr.*, 2008, **64**, 112.

31 (a) Z. P. Demko, K. B. Sharpless, *Org. Lett*., 2001, **3**, 4091; (b) Z. P. Demko, K. B. Sharpless, *Angew. Chem., Int. Ed*. 2002, **41**, 2110; (c) F. Himo, Z. P. Demko, L. Noodleman and K. B. Sharpless, *J. Am. Chem. Soc*., 2003, **125**, 9983.

32 (a) S. Aoki, M. Zulkefeli, M. Shiro, M. Kohsako, K. Takeda and E. Kimura, *J. Am. Chem. Soc.,* 2005, **127**, 9129; (b) G. D. Santis, L. Fabbrizzi, M. Licchelli, A. Poggi and A. Taglietti, *Angew. Chem. Int. Ed. Engl.,* 1996, **35**, 202; (c) Z. Chang, A. S Zhang, T. L. Hu and X. H. Bu, *Cryst. Growth Des.,* 2009, **9**, 4840; (d) T. L. Hu, Y. Tao, Z. Chang and X. H. Bu, *Inorg. Chem.,* 2011, **50**, 10994.

33 (a) F. W€urthner, A. Sautter, *Chem. Commun.,* 2000, **6**, 445; (b) H. V. Rasika Dias, H. V. K. Diyabalanage, M. A. Rawashdeh Omary, M. A. Franzman and M. A. Omary, *J. Am. Chem. Soc.,* 2003, **125**, 12072;. (c) E. Cariati, X. H. Bu and P. C. Ford, *Chem. Mater.,* 2000, **12**, 3385; (d) D. M. Ciurtin, N. G. Pschirer, M. D. Smith, U. H. F. Bunz and H. C. Z. Loye, *Chem. Mater.,* 2001, **13**, 2743; (e) Y. B. Dong, H. Y. Wang, J. P. Ma, D. Z. Shen and R. Q. Huang, *Inorg. Chem.,* 2005, **44**, 4679; (f) P. D. Harvey, H. B. Gray, *J. Am. Chem. Soc.,* 1988, **110**, 2145; (g) V. W. W. Yam, K. K. W. Lo, *Chem. Soc. Rev.,* 1999, **28**, 323; (h) C. Seward, W. L. Jia, R. Y. Wang, G. D. Enright and S. Wang, *Angew. Chem. Int. Ed.,* 2004, **43**, 2933; (i) C. D. Wu, H. L. Ngo and W. Lin, *Chem. Commun.,* 2004, **14**, 1588, (j) Y. J. Cui, Y. F. Yue G. D. Qian and B. L. Chen, *Chem. Rev.,* 2012, **112**, 1126.

34 (a) K. Liu, B. H. Ma, X. L. Guo, D. X. Ma, L. K. Meng, G. Zeng, F. Yang, G. H. Li, Z. Shi and S. H. Feng, *CrystEngComm*, 2015, 1**7**, 5054; (b) X. Y. Wan, F. L. Jiang, L. Chen, J. Pan, K. Zhou, K. Z. Su, J. D. Pang, G. X . Lyu and M. C. Hong, *CrystEngComm,* 2015, **17**, 3829.

35 (a) H. Wu, W. Dong, H. Y. Liu, J. F. Ma, S. L. Li, J. Yang, Y. Y. Liu and Z. M. Su, *Dalton Trans.,* 2008, **39**, 5331; (b) R. H. Wang, D. Q. Yuan, F. L. Jiang, L. Han, Y. Q. Gong and M. C. Hong, *Cryst. Growth Des*., 2006, **6**, 1351.

36 (a) C. A. Bauer, T. V. Timofeeva, T. B. Settersten, B. D. Patterson, V. H. Liu, B. A. Simmons and M. D. Allendorf, *J. Am. Chem. Soc*., 2007, **129**, 7136.

Captions to Figures

Fig. 1. View of **(a)** the coordination environment of the Zn center in **1**, symmetry code: **a**: -x+2,y-1/2,-z+1/2; **b**: -x+2,-y,-z; **(b)** the dinuclear units $[Zn_2(HL^1)_2]$ units in **1**; **(c)** the 2D coordination layers of **1**; **(d)** the 2D four connected $\{4^4\cdot6^2\}$ topological network (H atoms omitted for clarity).

Fig. 2. View of **(a)** the coordination environment of the Zn1 center in **2**, symmetry code: **c**: x-1/2,-y+3/2,z-1/2; **d**: -x,-y+1,-z+1; **x:** x+1/2,-y+3/2,z+1/2; **(b)** the dimeric units $[ZnN_4]_2$ unit in **2**; **(c)** the 2D coordination layers of **2** (H atoms omitted for clarity).

Fig. 3. View of **(a)** the coordination environment of the Cd1 center in **3**, symmetry code: **e**: -x+5/3,-y+4/3,-z+1/3; **f**: -x+y+4/3,-x+5/3,z-1/3; **g**: y,-x+y+1,-z; **(b)** the -Cd1-tetrazole-Cd1- helical chains extending along the *b* axis in **3**; **(c)** the coordination environment of the Cd2 center in **3**, symmetry code: **h**: -x+5/3,-y+4/3,-z+1/3; **(d)** the Cd2 centers formed a 1-D chain structure bridged by the ligands HL^1 in **3**; **(e)** the 3D framework formed by the SBUs $[Cd_3Cl_2]$; **(f)** the 3D 10-connected net with $\{3^{18}\cdot4^{18}\cdot5^9\}$ topology of **3** (H atoms omitted for clarity).

Fig. 4. View of the coordination environment of Cd(II) ions in **4**, symmetry code: **i**: -x,-y+1,-z.

Fig. 5. View of **(a)** the coordination environment of the Cd1 center in **5**, symmetry code: **j**: -x+1,y,-z+1/2; **k**: -x+1,-y+1,-z; **l**: x,-y+1,z+1/2; **m**: x,-y+2,z+1/2; **n**: -x+1,-y+2,-z; **(b)** 1-D chain formed via the coordination between the Cd1 centers and the ligands HL^1 in **5**; **(c)** the coordination environment of the Cd2 center in **5**, symmetry code: **o**: -x+3/2,-y+3/2,-z; **p**: -x+3/2,y-1/2,-z+1/2; **(d)** the Cd2 centers form a 2-D sheet structure bridged by the ligands HL^1 in **5**; **(e)** the structure of **5** is assembled into 3-D network; **(f)** the 3D (6, 8)-connected net with $\{3^6\cdot4^6\cdot5^3\}\{3^6\cdot4^8\cdot5^4\cdot6^8\cdot7^2\}$ topology of **5** (H atoms omitted for clarity).

Fig. 6. View of **(a)** the coordination environment of the Zn^{II} ions in **6**, symmetry code: **r**: -x+2,-y+2,-z+1; **(b)** the dinuclear $[Zn_2N_4]$ units in **6**; **(c)** the 2D coordination layers of **6** (H atoms omitted for clarity).

Fig. 7. View of **(a)** the coordination environment of the Zn1 center in **7**, symmetry code: **s**: x,-y+5/2,z; **t**: x+1/2,y,-z+3/2; **(b)** the Zn1 centers form a 1-D chain structure bridged by the ligands HL^2 and N_3^- in **7**; **(c)** the Zn1 centers form a 2-D sheet structure bridged by the ligands HL^2 and N_3 in **7**; **(d)** the coordination environment of the Zn2 center in **5**, symmetry code: **t**: x − y, x, 1 − z; b: x, y, 1 + z; **(e)** the 2D coordination layer of **7** (H atoms omitted for clarity).

Fig. 8. View of the coordination environment of Cd(II) ions in **8**.

Fig. 9. View of **(a)** the coordination environment of the Cd1 center in **9**, symmetry code: **u**: -x+2,-y,-z; **v**: -x+2,y+1/2,-z+1/2; **w**: -x+2,-y+1,-z; **(b)** the Cd1 centers form a 2-D sheet structure bridged by the ligands H$\mathbf{L}^{2}$ in **9**; **(c)** the coordination environment of the Cd2 center in **9**; **(d)** the Cd1 centers form 1D helical chains extending in **9**; **(e)** the $[Cd_4(OH)_2(H_2O)_2(NO_3)_2]$ clusters structure in **9**; **(f)** the 2D sheet structure of **9**; **(g)** the two dimensional six-connected $\{3^6\cdot4^6\cdot5^3\}$ topological network of **9** (H atoms omitted for clarity).

Fig. 10. View of **(a).** emission spectra of **1**–**5**, as well as the free ligand $H_3\mathbf{L}^{1}$ in the solid state at ambient temperature. **(b)**. emission spectra of **6**–**9**, as well as the free ligand $H_3\mathbf{L}^{2}$ in the solid state at room temperature.

Table **1.** Crystal Data and Structure Refinement Summary for complexes **1~9**

Complexes	**1**	**2**	**3**	**4**	**5**
Formula	$C_4H_7N_9OZn$	$C_4H_5N_9Zn$	$C_8H_{10}N_{18}Cl_2Cd_3$	$C_8H_{22}N_{18}O_6Cd_2$	$C_8H_{12}N_{18}OCd_2$
Formular wt	262.54	244.53	766.44	691.20	601.12
Crystal System	Monoclinic	Monoclinic	Hexagonal	Monoclinic	Monoclinic
Space group	*P2(1)/c*	*P2(1)/n*	*R-3*	*P2(1)/n*	*C2/c*
T/K	296(2)	296(2)	296(2)	296(2)	296(2)
a/Å	6.843(11)	7.776(4)	27.148(4)	7.7937(6)	21.6492(7)
b/Å	7.155(11)	13.987(6)	27.148(4)	14.2172(12)	9.9528(3)
c/Å	17.08(3)	8.352(4)	9.957(3)	10.3075(8)	8.4146(3)
α/deg	90	90	90	90	90
β/deg	93.79(2)	101.601(11)	90	100.571(2)	105.5970(10)
γ/deg	90	90	120	90	90
V/Å^3	834(2)	889.8(7)	6355(2)	1122.73(16)	1746.33(10)
Z	4	4	9	2	4
D/g cm^{-3}	2.075	1.826	1.802	2.045	2.286
μ/mm^{-1}	2.934	2.736	2.457	1.962	2.484
F(000)	520	488	3258	680	1160
Messured reflns	1024	7149	12392	9025	7060
Obsd reflns	750	2230	2547	2869	2172
R^a/wR^b	0.0524/0.1358	0.0488/0.1190	0.0211/0.0569	0.0243/0.0629	0.0222/0.0644

Complexes	**6**	**7**	**8**	**9**
Formula	$C_6H_9N_9Zn$	$C_6H_9N_{12}ClZn_2$	$C_6H_{15}N_9O_3Cd$	$C_6H_{12}N_{10}O_5Cd_2$
Formular wt	272.59	415.45	373.65	529.05
Crystal system	Monoclinic	Orthorhombic	Monoclinic	Monoclinic
Space group	*P2(1)/n*	*Pnma*	*Cc*	*P2(1)/c*
T/K	296(2)	296(2)	296(2)	296(2)
a/Å	8.2145(5)	6.8924(3)	13.4767(15)	10.6856(6)
b/Å	12.2263(7)	10.0600(4)	7.5845(9)	7.3274(4)
c/Å	10.0212(6)	19.7902(8)	12.9148(14)	18.8986(11)
α/deg	90	90	90	90
β/deg	102.7770(10)	90	99.542(2)	105.7760(10)
γ/deg	90	90	90	90
V/Å^3	981.54(10)	1372.20(10)	1301.8(3)	1423.98(14)
Z	4	4	4	4
D/g cm^{-3}	1.845	2.006	1.907	2.468
μ/mm^{-1}	2.490	3.704	1.700	3.032
F(000)	552	820	744	1016
Messured reflns	6189	10913	5209	11418
Obsd reflns	1737	1811	2335	3544
R^a/wR^b	0.0226/0.0549	0.0294/0.0792	0.0181/0.0480	0.0164/ 0.0374

[a] $R = \Sigma(||F_0|-|F_C||)/\Sigma|F_0|$; [b] $wR = [\Sigma w(|F_0|^2-|F_C|^2)^2/\Sigma w(F_0^2)]^{1/2}$

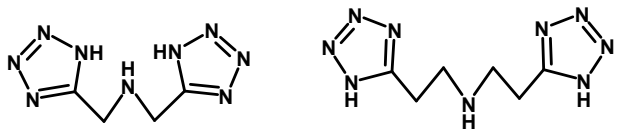

H_3L^1 H_3L^2

Scheme 1 The tetrazole ligands studied in this work.

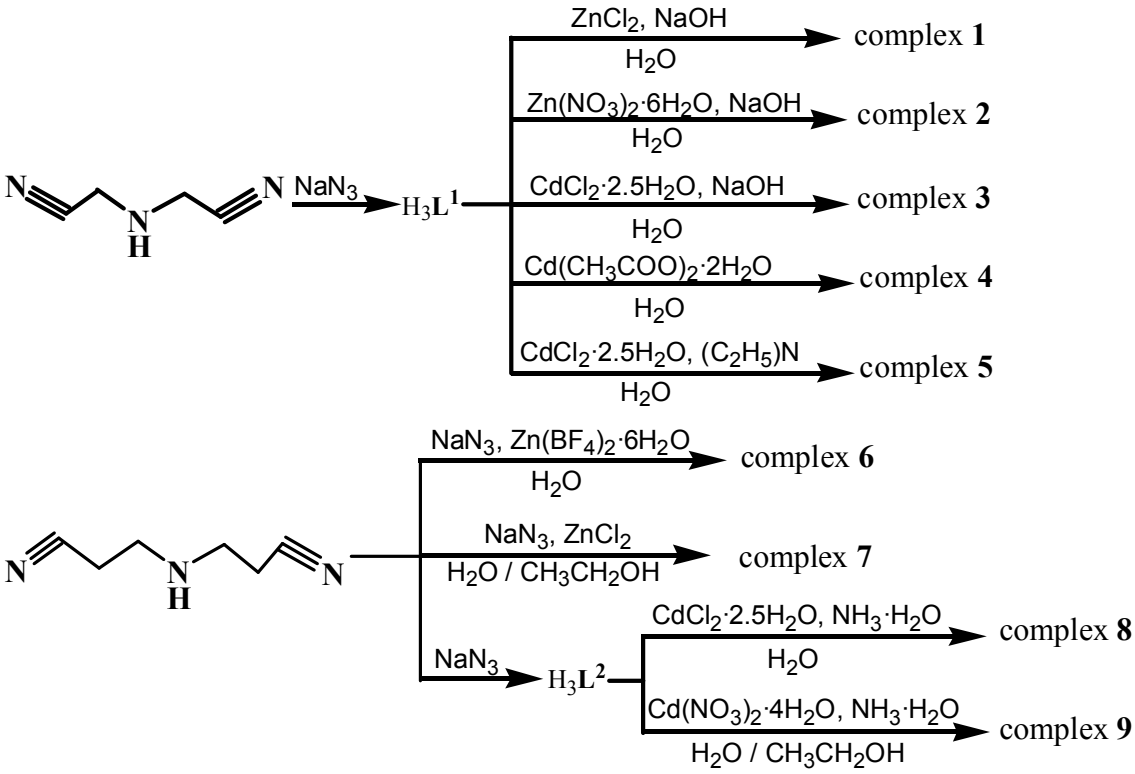

Scheme 2 The synthetic route of tetrazole-based complexes **1**-**9**.

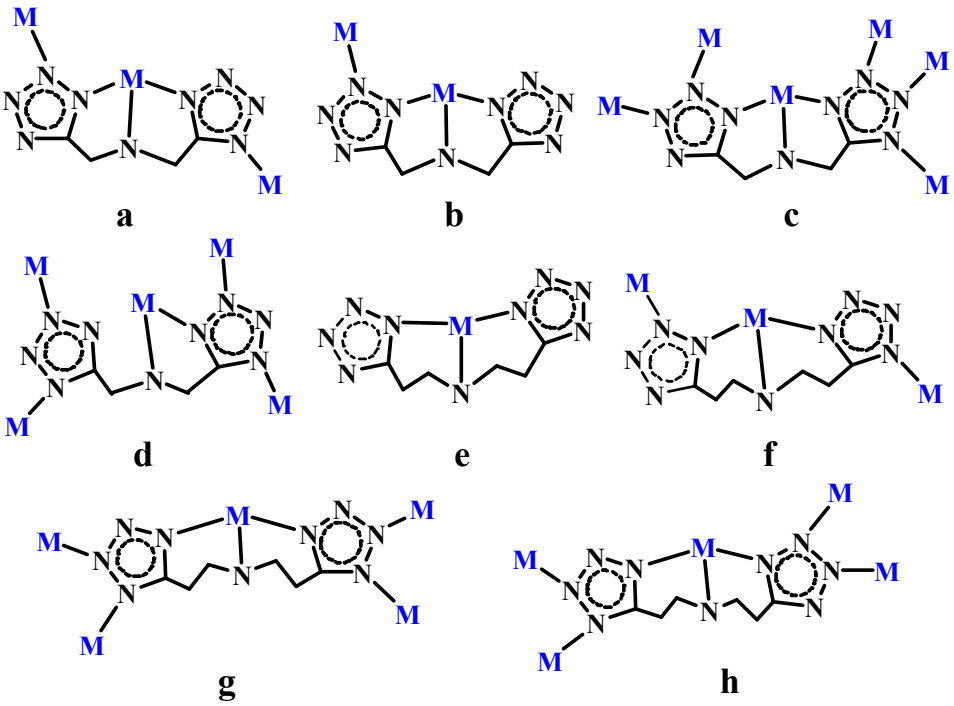

Scheme 3 Coordination modes of the ligands $H_3\mathbf{L}^1$ and $H_3\mathbf{L}^2$ observed in this work.

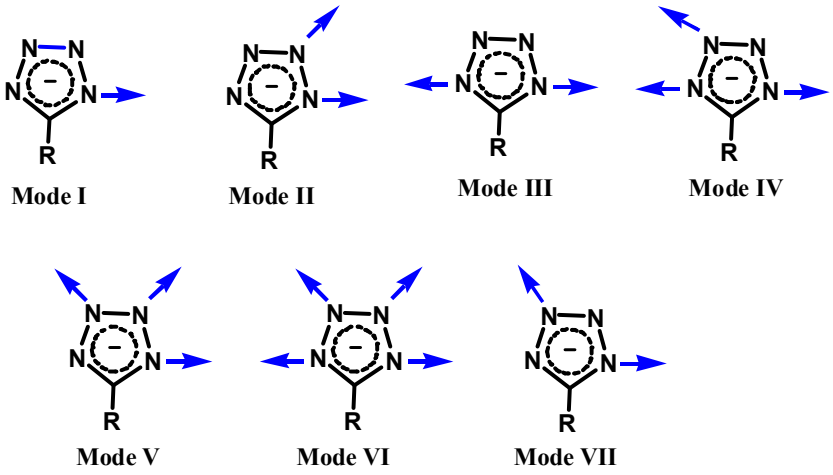

Scheme 4 The coordination modes of tetrazole found in this work.

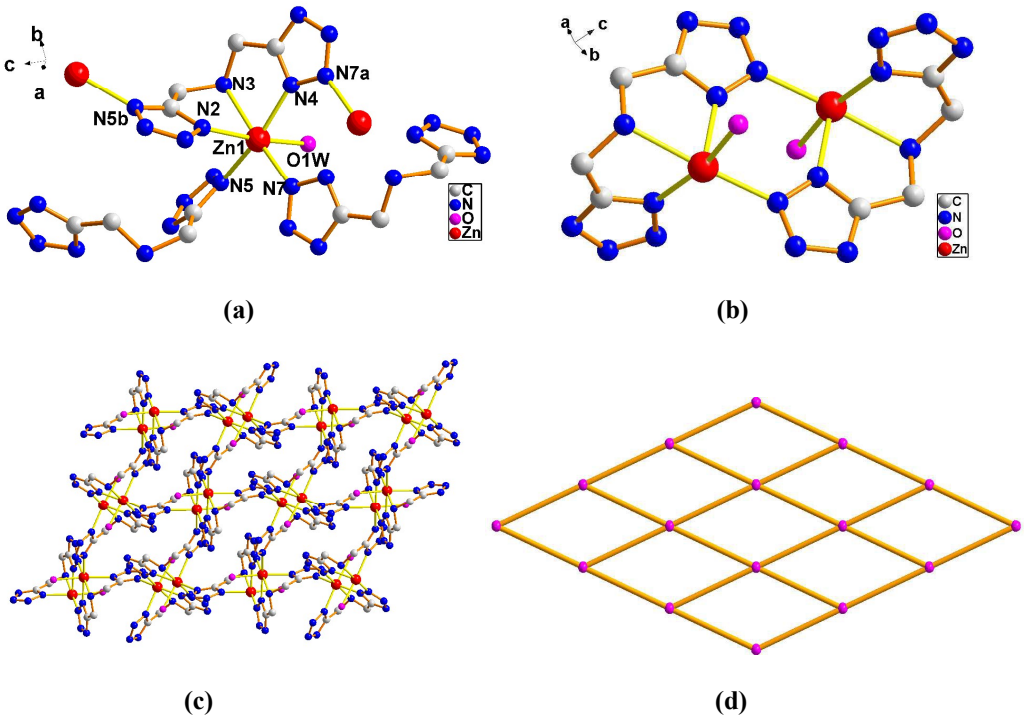

(a) (b)

(c) (d)

Fig. 1

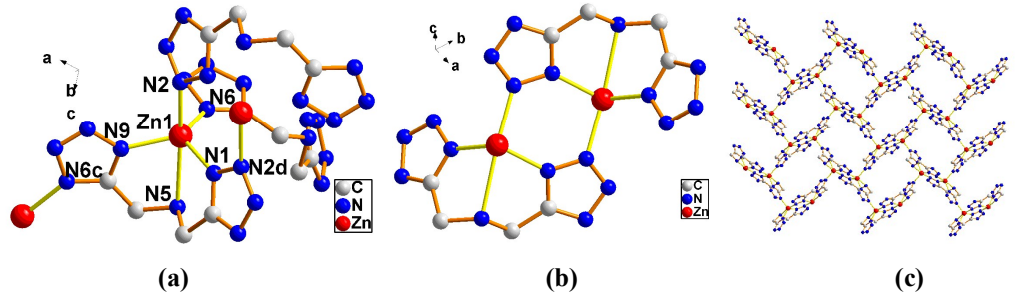

(a) (b) (c)

Fig. 2

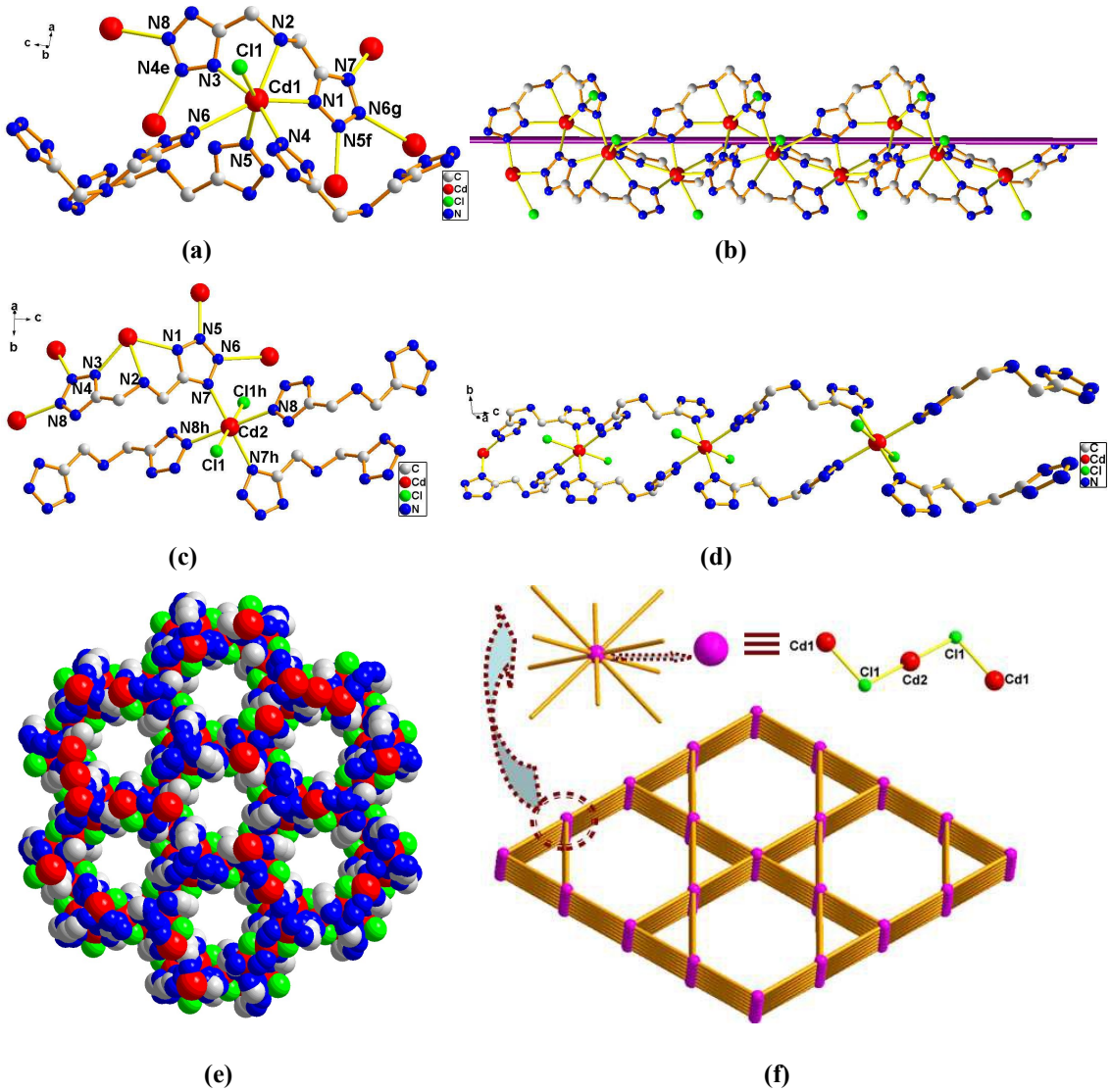

Fig. 3

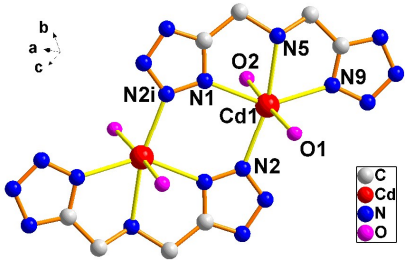

Fig. 4

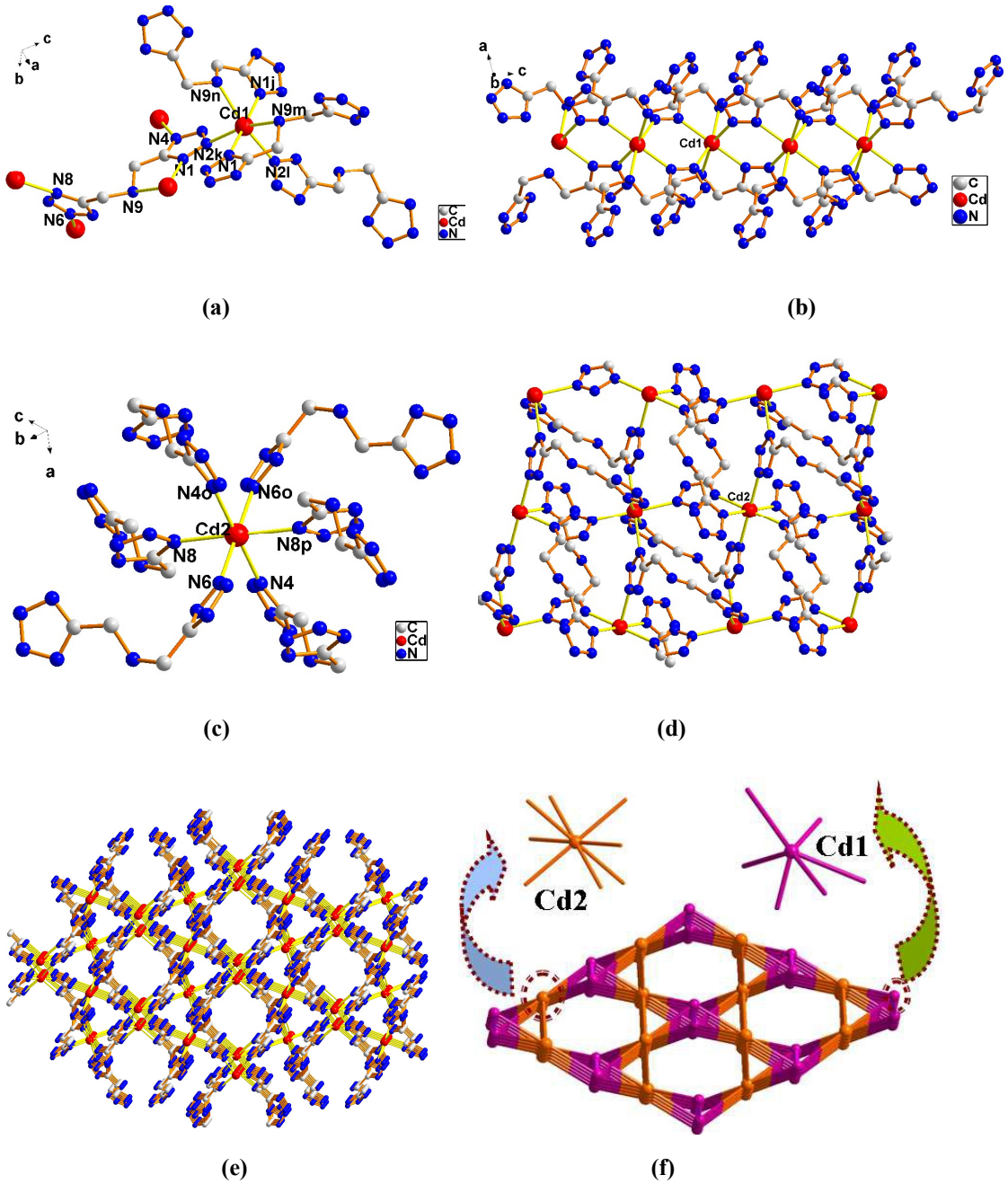

(a) (b)

(c) (d)

(e) (f)

Fig. 5

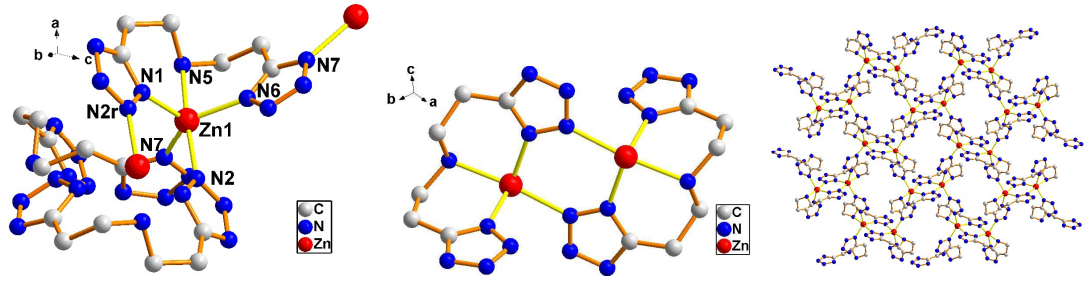

(a) (b) (c)

Fig. 6

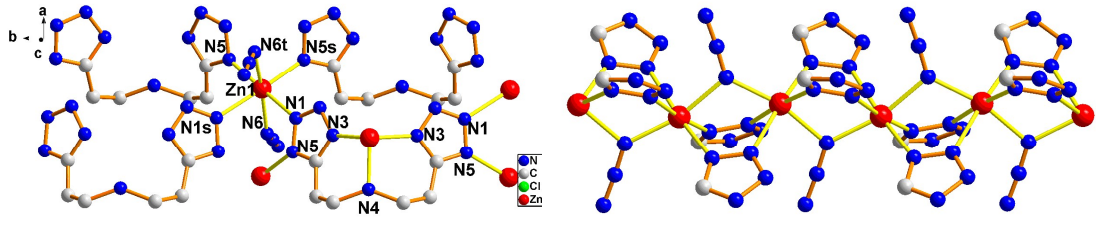

(a) (b)

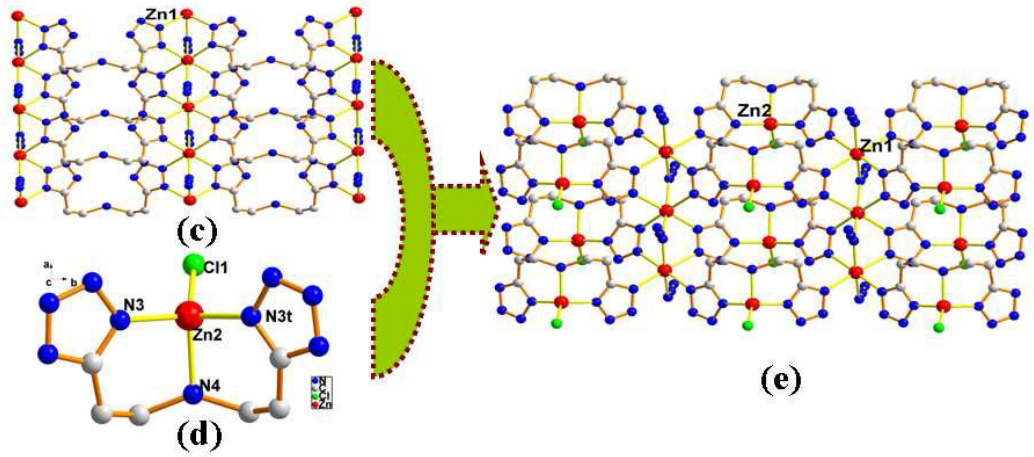

Fig. 7

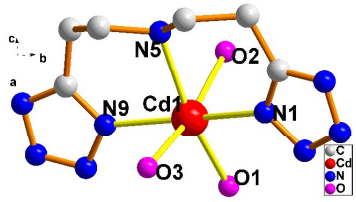

Fig. 8

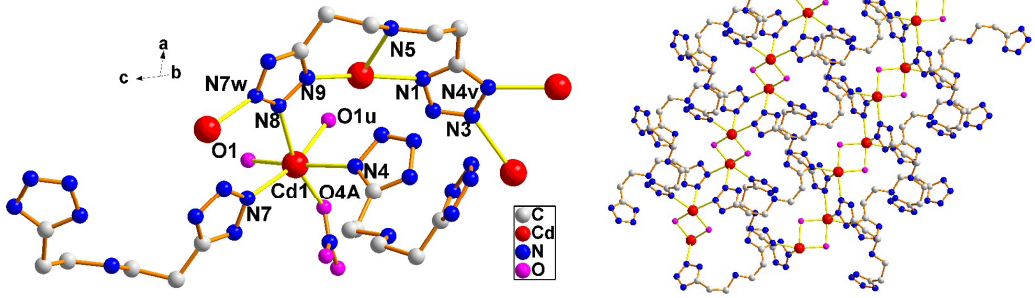

(a) (b)

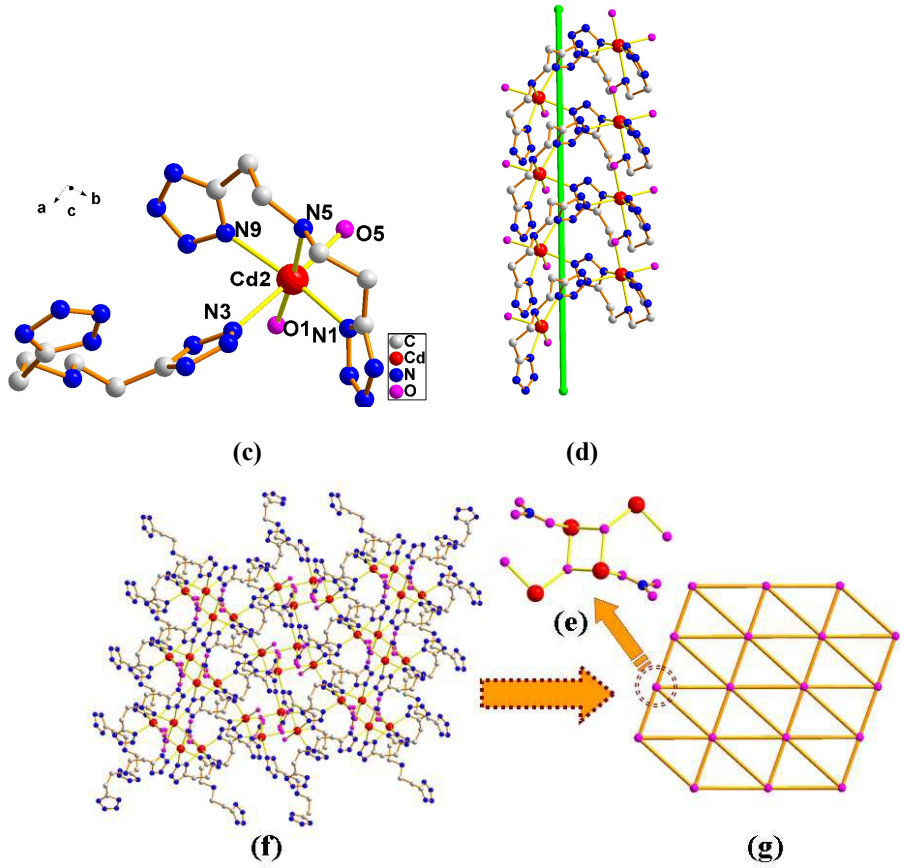

Fig. 9

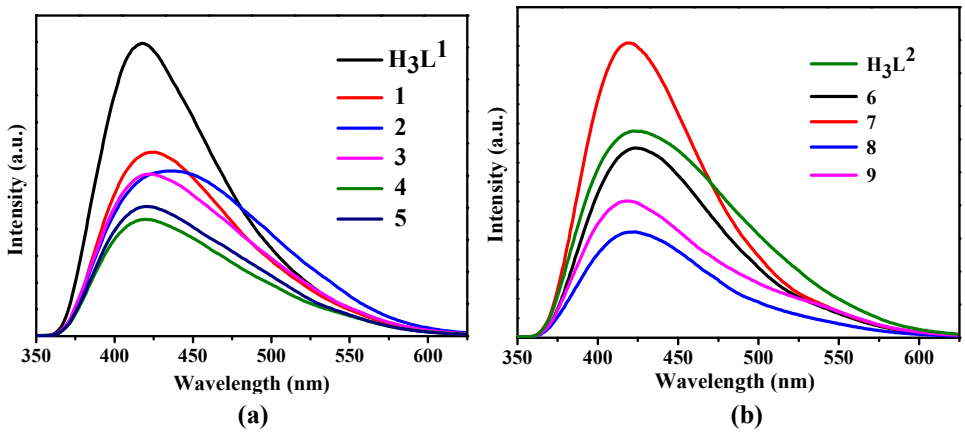

Fig. 10

Graphical Abstract

Zinc and cadmium complexes based on bis-(1*H*-tetrazol-5-ylmethyl/ylethyl)-amine ligands: structures and photoluminescence properties

Duo-Zhi Wang, Jian-Zhong Fan, Dian-Zeng Jia and Ceng-Ceng Du

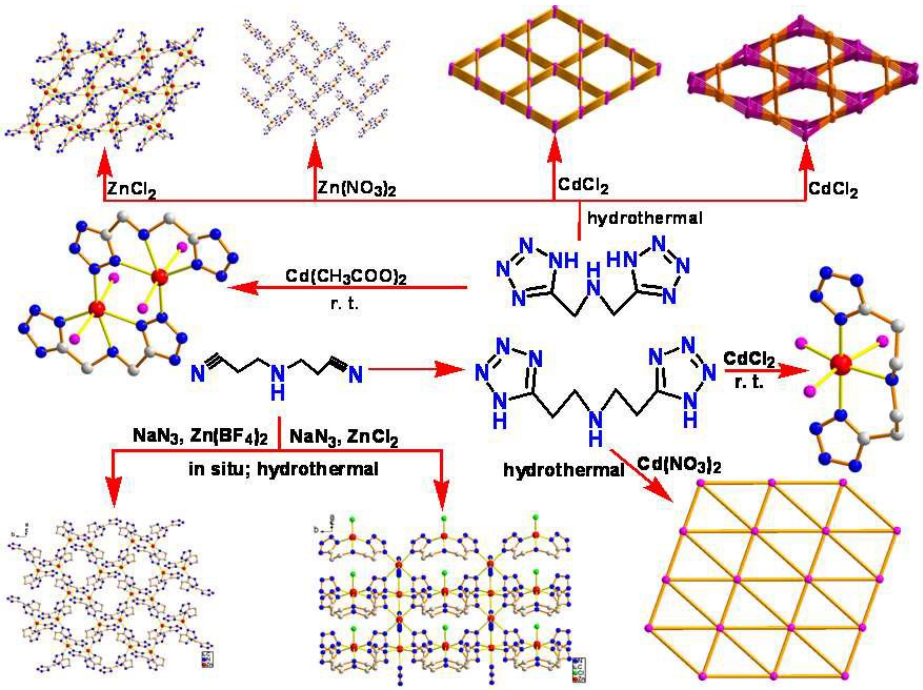

In efforts to explore the effects of metal ions, ligand structures, counter-anions on the structures and properties of metal-organic complexes, nine zinc and cadmium coordination compounds with bis-(1*H*-tetrazol-5-ylmethyl/ylethyl)-amine were synthesized and structurally characterized by elemental analyses, IR spectroscopy and single-crystal X-ray diffraction. All the complexes are air stable at room temperature. Furthermore, the fluorescent emission and fluorescence lifetime of complexes **1**–**9** have been investigated and discussed.